New Zealand Journal of Geology and Geophysics

ISSN: (Print) (Online) Journal homepage: www.tandfonline.com/journals/tnzg20

Ruapehu and Tongariro stratovolcanoes: a review of current understanding

Graham S. Leonard, Rosie P. Cole, Bruce W. Christenson, Chris E. Conway, Shane J. Cronin, John A. Gamble, Tony Hurst, Ben M. Kennedy, Craig A. Miller, Jonathan N. Procter, Leo R. Pure, Dougal B. Townsend, James D. L. White & Colin J. N. Wilson

To cite this article: Graham S. Leonard, Rosie P. Cole, Bruce W. Christenson, Chris E. Conway, Shane J. Cronin, John A. Gamble, Tony Hurst, Ben M. Kennedy, Craig A. Miller, Jonathan N. Procter, Leo R. Pure, Dougal B. Townsend, James D. L. White & Colin J. N. Wilson (2021) Ruapehu and Tongariro stratovolcanoes: a review of current understanding, New Zealand Journal of Geology and Geophysics, 64:2-3, 389-420, DOI: 10.1080/00288306.2021.1909080

To link to this article: https://doi.org/10.1080/00288306.2021.1909080

Published online: 02 May 2021.

NEW ZEALAND JOURNAL OF GEOLOGY AND GEOPHYSICS
2021, VOL. 64, NOS. 2–3, 389–420
https://doi.org/10.1080/00288306.2021.1909080

Taylor & Francis
Taylor & Francis Group

REVIEW ARTICLE

OPEN ACCESS Check for updates

Ruapehu and Tongariro stratovolcanoes: a review of current understanding

Graham S. Leonard [a], Rosie P. Cole [b], Bruce W. Christenson[a], Chris E. Conway[c], Shane J. Cronin [d], John A. Gamble[e,f], Tony Hurst[a], Ben M. Kennedy[g], Craig A. Miller [a], Jonathan N. Procter[h], Leo R. Pure[e], Dougal B. Townsend[a], James D. L. White [b] and Colin J. N. Wilson [e]

[a]GNS Science, Avalon Research Centre, Lower Hutt, New Zealand; [b]Geology Department, University of Otago, Dunedin, New Zealand; [c]Research Institute of Earthquake and Volcano Geology, Geological Survey of Japan, National Institute of Advanced Industrial Science and Technology, Tsukuba; [d]School of Environment, The University of Auckland, Auckland, New Zealand; [e]School of Geography, Environment and Earth Sciences, Victoria University of Wellington, Wellington, New Zealand; [f]School of Biological, Earth and Environmental Sciences, University of Cork, Ireland; [g]School of Earth and Environment, University of Canterbury, Christchurch, New Zealand; [h]Volcanic Risk Solutions, Institute of Agriculture and Environment, Massey University, Palmerston North, New Zealand

ABSTRACT

Ruapehu (150 km^3 cone, 150 km^3 ring-plain) and Tongariro (90 km^3 cone, 60 km^3 ring-plain) are iconic stratovolcanoes, formed since ~230 and ~350 ka, respectively, in the southern Taupo Volcanic Zone and Taupo Rift. These volcanoes rest on Mesozoic metasedimentary basement with local intervening Miocene sediments. Both volcanoes have complex growth histories, closely linked to the presence or absence of glacial ice that controlled the distribution and preservation of lavas. Ruapehu cone-building vents are focused into a short NNE-separated pair, whereas Tongariro vents are more widely distributed along that trend, the differences reflecting local rifting rates and faulting intensities. Both volcanoes have erupted basaltic andesite to dacite (53–66 wt.% silica), but mostly plagioclase-two pyroxene andesites from storage zones at 5–10 km depth. Erupted compositions contain evidence for magma mixing and interaction with basement rocks. Each volcano has an independent magmatic system and a growth history related to long-term (>10^4 years) cycles of mantle-derived magma supply, unrelated to glacial/interglacial cycles. Historic eruptions at both volcanoes are compositionally diverse, reflecting small, dispersed magma sources. Both volcanoes often show signs of volcanic unrest and have erupted with a wide range of styles and associated hazards, most recently in 2007 (Ruapehu) and 2012 (Tongariro).

ARTICLE HISTORY
Received 3 June 2020
Accepted 24 March 2021

KEYWORDS
Stratovolcano; Ruapehu; Tongariro; Ngāuruhoe; eruption; andesite; magma system; lahar; sector collapse; structure; faulting

Introduction

Ruapehu and Tongariro volcanoes are two of the visually most prominent volcanic landforms of the Taupo Volcanic Zone (TVZ), located in the central North Island of New Zealand (Figure 1). These two volcanoes are treasured by New Zealanders and are of special significance to Māori (see Gabrielsen et al. 2017). The TVZ itself is the southernmost, continental part of the subduction-related arc stretching from New Zealand to Tonga (offshore called the Tonga-Kermadec arc: Cole and Lewis 1981). Volcanism and concurrent rifting along the active TVZ sector of the arc initiated at c. 2 Ma with the eruption of voluminous andesites, now buried, but penetrated by drilling at several geothermal fields in the central TVZ (e.g. Milicich et al. 2020). Prior to this time the arc, with a sub-parallel trend, passed through the Tauranga area, several tens of kilometres to the northwest. Over about 15 Myr, the arc has rolled back from intersecting the Coromandel Peninsula, through Tauranga to its current position, due to subduction slab steepening or rollback (Seebeck et al. 2014).

The TVZ is divisible into three segments. The northern and southern segments are dominated by andesitic volcanism and a central segment is dominated by extraordinarily vigorous rhyolitic volcanism (Wilson et al. 1995). The boundary between the central and southern segments of the TVZ lies just south of Lake Taupo. North of this transition there is a markedly higher rate of mantle melt supply into the central TVZ, leading to a higher heat flow and rates of magmatism and volcanism (Barker et al. 2020). Within the southern segment of the TVZ, mounts Tongariro (including the prominent Ngāuruhoe cone) and Ruapehu are two large andesite-dacite stratovolcano complexes that are central features of Tongariro National Park (TNP; Figures 2 and 3; Townsend et al. 2017). Coinciding and interacting with the TVZ is a similarly-sized and -orientated tectonic structure, the Taupo Rift (Villamor et al. 2017). Ruapehu and Tongariro lie within the southernmost extent of this rift, which is locally represented by nested grabens occupied by the two mountains and their ring-plains.

CONTACT Graham S. Leonard g.leonard@gns.cri.nz

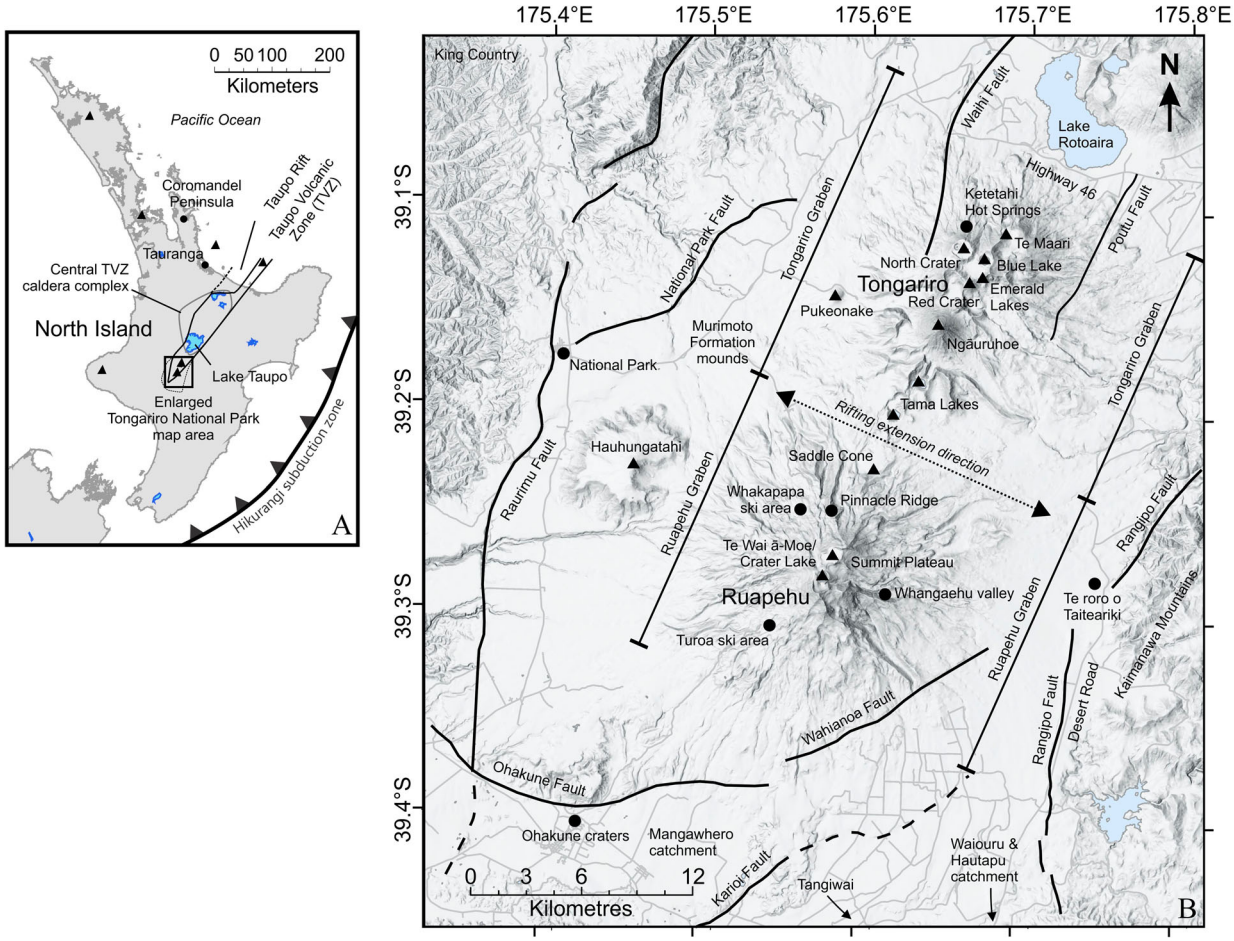

Figure 1. A: Location of the Taupo Volcanic Zone, coincident Taupo Rift and the volcanic centres (triangles) in the North Island of New Zealand. Box shows the area of panel B and maps in Figure 3. **B**: Hillshade map of Tongariro and Ruapehu stratovolcanoes, showing key locations (dots and arrows), faults (annotated lines) and eruptive vents (triangles) described in this paper.

Figure 2. Oblique aerial view of the Tongariro National Park area with Ruapehu and Tongariro stratovolcanoes, including the prominent Ngāuruhoe cone (Tongariro), looking south. The Waihi Fault splays are picked out by shadow on the right (west) side of Tongariro (white arrows). Ketetahi hot springs are labelled 'k'. Lake Rotoaira in the left foreground. GNS Science photo by Dougal Townsend.

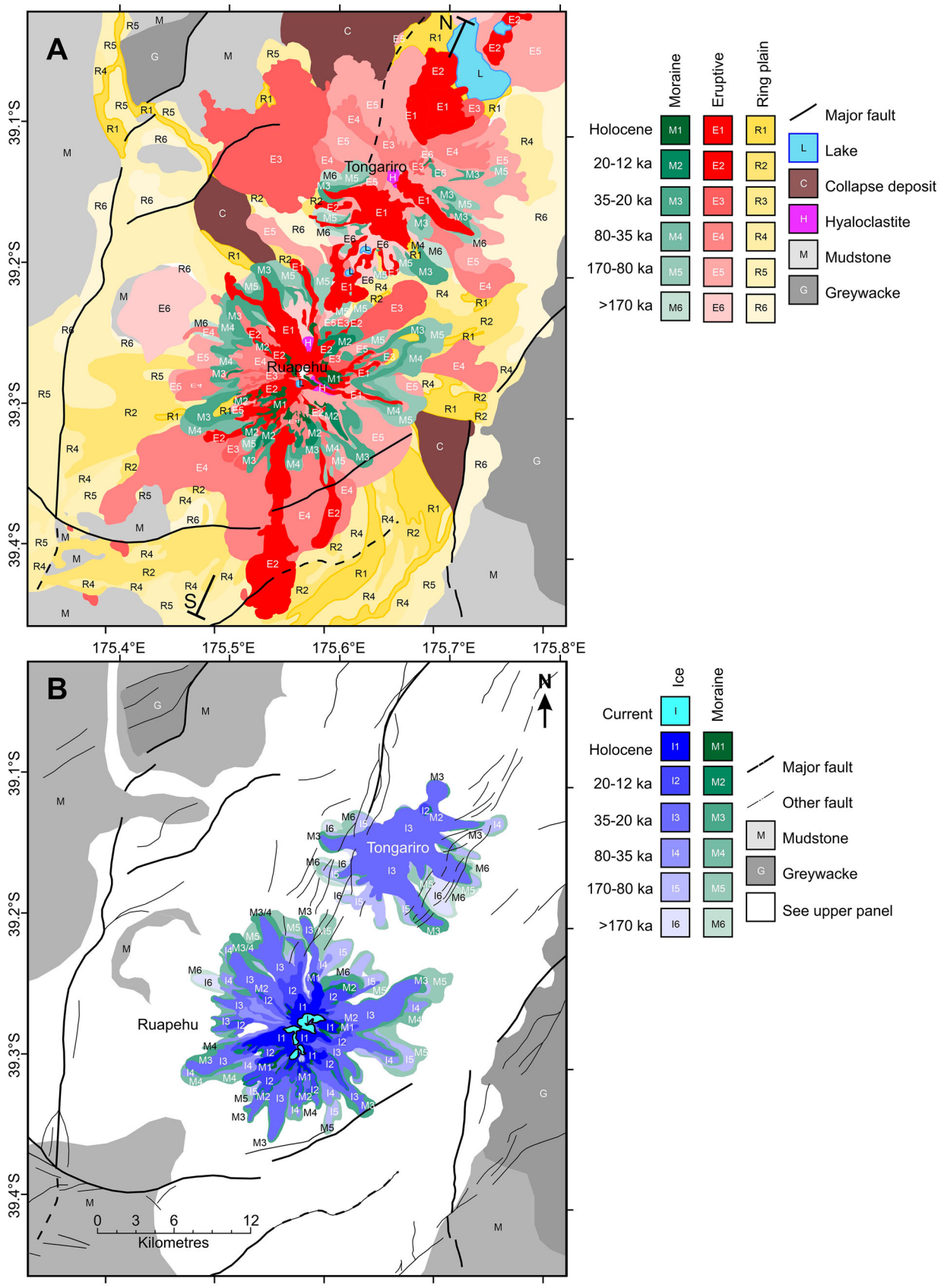

Figure 3. A: Simplified geological map of the Tongariro and Ruapehu edifices and ring plains, Cross sections in Figure 5 run along the line S-N; **B**: Glacial ice extent and moraines at the stratovolcanoes through time. Maps modified from Townsend et al. (2017). Key major faults are labelled on Figure 1.

The oldest recorded volcanism in the TNP area (933 ± 46 ka: Cameron et al. 2010) was at Hauhungatahi, northwest of Ruapehu. There is then a gap in dated materials until eruption of lava forming a small inlier on the western side of Tongariro that returned an age of 512 ± 59 ka (Pure et al. 2020).

The oldest dated materials associated directly with the Tongariro and Ruapehu edifices are around 350 and 200 ka, respectively (Gamble et al. 2003; Pure et al. 2020: see below) and activity has continued through to the present day. Numerous historic eruptions have occurred from Te Wai ā-Moe/Crater Lake on Ruapehu and multiple vents on Tongariro, most recently in 2007 and 2012, respectively. At Tongariro the most recent eruption was at the upper Te Maari crater, whereas previous historic events up to and including 1975 were mostly from Ngāuruhoe.

Although there are other andesite centres within and around the TNP to the north and northwest of Lake Rotoaira, these have little or no evidence of post-150 ka activity and are now covered in dense vegetation with virtually no rock exposure. Studied in much less detail, these centres are composed of andesites that are broadly similar in composition to those of Ruapehu and Tongariro but generally predate the growth of those cones (Cole 1978; Cashman 1979; Cole et al. 1983). We thus focus on Ruapehu and Tongariro here as the largest, most recently active and thus well studied centres.

This paper provides a review of the current state of geological and geophysical understanding of Ruapehu and Tongariro volcanoes, and references a wide range of TNP volcanic literature. The reader is also referred to Townsend et al. (2017), which includes a map and detailed text citing key publications related to many specific features and geological units of these volcanoes. A digital revision of Tongariro geological units based on Pure et al. (2020) is underway.

Geological context

Crustal structure beneath TNP

Tongariro National Park sits approximately 75 km above the subducting Pacific tectonic plate (Eberhart-Phillips et al. 2020) that ultimately drives volcanism in TNP through dehydration of the subducting slab, providing water to the overlying mantle and promoting melting and magmatism. This melting produces low V_p zones in the mantle wedge between the overlying and subducting plates, as seen in seismic tomographic reconstructions beneath the TNP and elsewhere along the TVZ (Reyners et al. 2006). However, tomography results show no low V_p zone southwest of Ruapehu. The absence of low V_p in the mantle wedge above the slab suggests that there is no upwards return flow in the mantle south of Ruapehu and likely explains why volcanism stops at Ruapehu (Reyners et al. 2006; Hurst et al. 2016).

Crustal seismicity indicates that the thickness of brittle crust is approximately 25 km beneath TNP (below which it is ductile), thickening to 40 km southwest of Ruapehu (Eberhart-Phillips et al. 2020). Deep crustal structure in the southern TVZ is characterised by a complex pattern of shear wave splitting orientations representing structural features such as faults or pockets of melt (Illsley-Kemp et al. 2019). Fast orientations, that are typically parallel to the trend of structural features, are N-S north of Tongariro, but change to E-W at Tongariro, change back to N-S beneath Ruapehu and then back again to E-W south of Ruapehu (Johnson et al. 2011; Illsley-Kemp et al. 2019). These variable orientations reflect the lesser influence of rifting and more influence of N-S and E-W fault sets at the southern end of the TVZ (Villamor and Berryman 2006; Illsley-Kemp et al. 2019).

Pre-volcanic (basement) geology

The pre-volcanic basement beneath Ruapehu and Tongariro consists of metamorphosed Triassic to Cretaceous rocks. A thin (<1–1.5 km) layer of non-metamorphosed Tertiary marine sediments sits on the basement surface beneath Ruapehu, but is probably not present beneath Tongariro. The metamorphic rocks at the surface are dominated by quartzo-feldspathic greywackes, which comprise the backbone of both main islands of New Zealand (Mortimer 2004). The Kaweka Terrane (Adams et al. 2009) crops out to the east of the park and forms the Kaimanawa Mountains, while the Waipapa (composite) Terrane crops out to the west (Beetham and Watters 1985; Mortimer et al. 1997).

Beneath Mt Tongariro, the greywacke basement top is modelled from gravity data as a continuous surface at around 0–500 m below sea level, dipping to the north (Miller and Williams-Jones 2016; Robertson and Davey 2018). Gravity models (Cassidy et al. 2009; Robertson and Davey 2018) suggest that the basement is shallowest (approximately at sea level) around the Tama Lakes area and deepens again beneath Ruapehu to 500–1000 m below sea level (Figure 4C). Seismic refraction studies to the south east of Ruapehu suggest that the basement becomes shallower (100–300 m above sea level) towards the eastern graben-bounding faults. Most models show the basement dipping gently (<5°) to the north and south away from the volcanoes, reaching maximum depths of 1000–1500 m below sea level at the termination of the TVZ (and Taupo Rift) to the south, and at the edge of Lake Taupo to the north (Figure 4C; Miller and Williams-Jones 2016; Robertson and Davey 2018).

Above the greywacke, the Tertiary sediments consist of mudstone plus minor sandstone and limestone that are exposed in the King Country hills to the west of the park. These sediments are locally preserved resting on Kaweka greywacke southeast of the park, but are not found on the top of the Kaimanawa Mountains suggesting that they have been eroded from higher areas (Browne 2004). The density and resistivity of

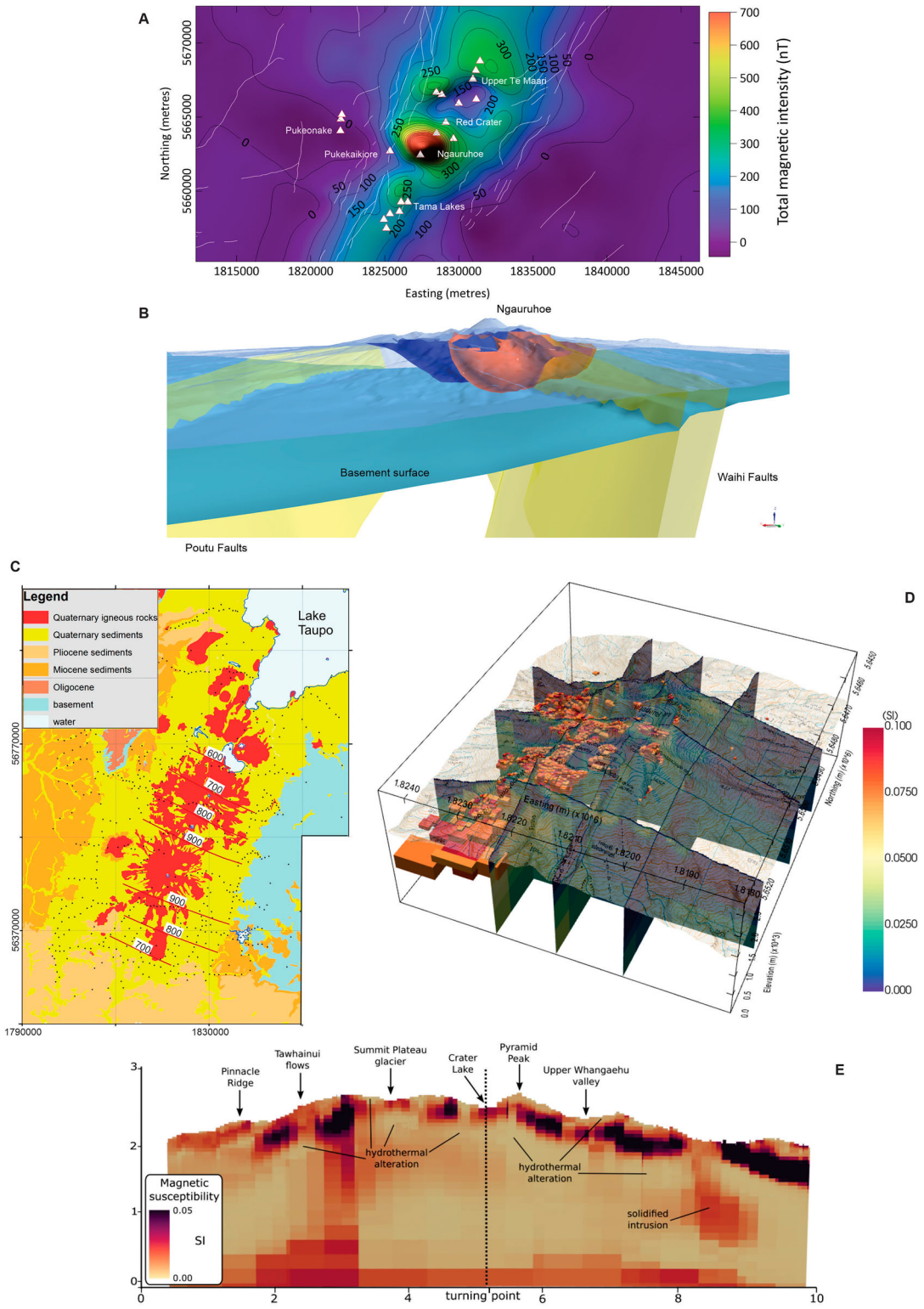

Figure 4. Summary geophysical data and models for the TNP stratovolcanoes. **A**: Reduced to pole, total magnetic intensity anomaly for Tongariro; modified from Miller and Williams-Jones (2016). **B**: a model of the extent of the hydrothermal system as revealed by magnetic and gravity data, looking south-southwest; red is low density hydrothermal alteration, blue is low magnetisation hydrothermal alteration, the grey lower surface represents the greywacke basement derived from gravity data; modified from Miller and Williams-Jones (2016). **C**: Depth to the basement (red contours in hundreds of metres) as determined by gravity data. Basement depth shown as contour lines overlain on simplified geological map. Reproduced with permission from Robertson and Davey (2018). **D** and **E**: 3D model and cross section showing magnetic susceptibility distribution at Ruapehu. High magnetic susceptibility bodies are inferred as lava and intrusions, while low magnetic susceptibilities indicate alteration. 'D' model modified from Miller et al. (2020), 'E' Modified from Kereszturi et al. (2020).

these sediments are similar to overlying altered volcanic rocks, making them difficult to isolate in gravity (Miller and Williams-Jones 2016) and magnetotelluric (MT) models (Ingham et al. 2009) beneath the volcanoes. They have good resistivity contrast with unaltered volcanic rock, however, and, away from the volcanoes, they also have good density and resistivity contrasts with the basement greywacke. Southeast of Ruapehu, the velocity contrast of the sediments has allowed them to be imaged by seismic refraction (Sissons and Dibble 1981) as a 300–400 m thick layer between surface volcaniclastic rocks and basement greywacke. MT models suggest that these sediments exist beneath Ruapehu; they are not included in MT models north of Tama Lakes, however (Ingham et al. 2009; Hill et al. 2015).

Cassidy et al. (2009) combined modelling of gravity, MT and aeromagnetic data to delineate a low density, low- to intermediate-resistivity and non-magnetised layer interpreted as Tertiary sediments that range in thickness from tens to hundreds of metres beneath the Tama Lakes area. An upper magnetised layer, interpreted as the overlying volcanic deposits, is 800 m thick in the saddle between Tongariro and Ruapehu (Figure 5; Cassidy et al. 2009).

Structure and faulting

Ruapehu and Tongariro lie within major graben structures that form part of the Taupo Rift, a NNE-oriented, southward propagating continental intra-arc structure, active since c. 2 Ma (Rowland and Sibson 2001; Villamor et al. 2017; Milicich et al. 2020). The TVZ (defined from vent locations) and the Taupo Rift (defined from faulting) are approximately coincident, such that the TNP volcanoes lie within the southern limits of the rift, where faulting was initiated at c. 350 ka (Villamor et al. 2017). Within the TNP area, the Taupo Rift is divided into two segments, the Tongariro Graben and the Ruapehu

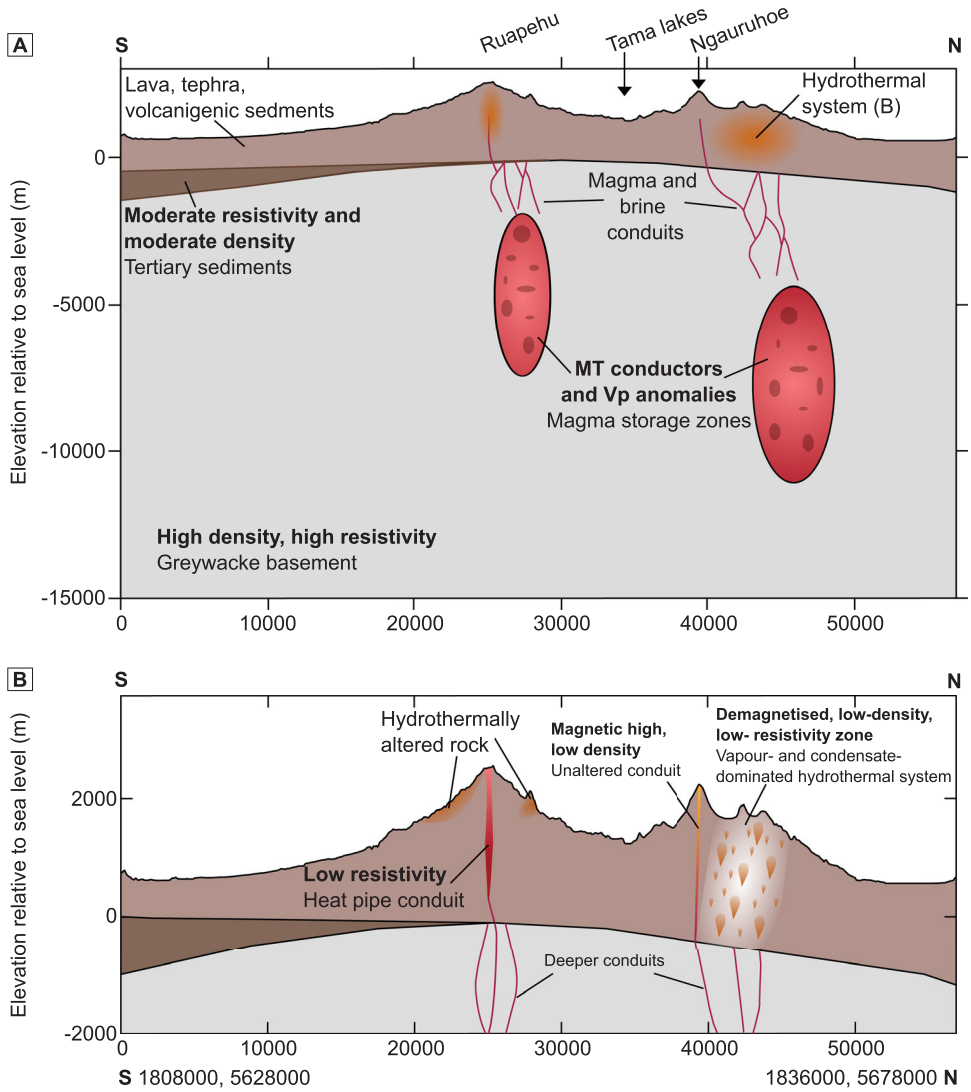

Figure 5. Deep (**A**) and shallow (**B**) schematic NNE-SSW cross sections summarising the subsurface structure and features as inferred from geophysical data (based largely on: Cassidy et al. 2009; Godfrey et al. 2017; Hill et al. 2015; Ingham et al. 2009; Jones et al. 2008; Kereszturi et al. 2020; Kilgour et al. 2013; Miller and Williams-Jones 2016; Miller et al. 2020; Rowlands et al. 2005). Geophysical information in bold text and geological interpretation in plain text. Line of sections shown in Figure 3.

Graben, within which the vents of Tongariro and Ruapehu volcanoes are respectively situated. These grabens are bounded by the NNE-oriented Waihi and Poutu normal fault zones (Tongariro) and National Park and Rangipo Faults (Ruapehu). Notable faults and fault zones are labelled in Figure 1. They are truncated in the south by the east–west oriented Ohakune Fault (Villamor and Berryman 2006; Gómez-Vasconcelos et al. 2017).

Regional and local tectonics play an important role in the vent locations across the two centres (Nairn et al. 1998; Conway 2016; Conway et al. 2018; Heinrich et al. 2020a; Pure 2020). At Tongariro, vents are distributed along a linear zone from Te Maari craters in the northeast to Tama Lakes in the southwest. In five out of seven eruptive episodes at Tongariro during a particularly active and explosive period from ~11.3 to 11.1 ka multiple vents appear to have been active at once, with eruptions progressing from north to south throughout each episode (Heinrich et al. 2020b). Pukeonake, ~6 km west of the linear vent zone, is considered to be a satellite vent. In contrast, Ruapehu vents are aligned along a narrower and shorter NNE-oriented corridor extending from Saddle Cone in the north, across the summit plateau to at least the Te Wai ā-Moe/Crater Lake vent area in the south (Figure 1). Ruapehu eruptions since 10 ka have been exclusively from two closely-spaced vents beneath the Summit Plateau and Te Wai ā-Moe/Crater Lake, with activity confined to the latter since about 2.5 ka (Donoghue et al. 1997).

Using aeromagnetic and gravity data, Cassidy et al. (2009) modelled a NW-SE cross-section south of Ngāuruhoe and proposed a zone of higher-density volcanic rocks coinciding with the position of the Waihi Fault. They inferred that the faults beneath the volcanoes have acted as conduits for magma and suggest that diking has contributed to extension. Three-dimensional models derived from more recent additional gravity data and new 3D interpretations of the aeromagnetic data (Miller and Williams-Jones 2016; Figures 4D and 4E) do not, however, show resolvable dikes along the intra-rift faults. The faults are interpreted as dominantly tectonic structures, while shallow magma storage zones or transport pathways are too small to resolve through geophysics. Away from the volcanoes, repeating earthquake swarms at Waiouru and National Park occur on rift bounding faults and are of tectonic origin. These earthquakes are associated with (aqueous) fluid movement but may be modulated by local stress changes caused by magma intrusion (Hurst and McGinty 1999, Hayes et al. 2004; Hamling et al. 2016; Hurst et al. 2018).

Gómez-Vasconcelos et al. (2017) combined models for fault dislocation related to diking with displacement measurements of faults in the Tongariro Graben to further show that extension is mostly related to tectonic activity. Extension rates of 7.0 ± 1.2 mm/yr since 20 ka were determined from a mean vertical slip rate of 6.2 ± 0.6 mm/yr along the faults. Of this extension, 78-95% is amagmatic while the remainder is coupled with diking (Gómez-Vasconcelos et al. 2017). A total subsidence of 500–700 m is estimated on the basement faults from geophysical models (Cassidy et al. 2009; Miller and Williams-Jones 2016). The late Quaternary extension rate across the faults of the Ruapehu Graben is 2.3 ± 1.2 mm/yr, with a subsidence rate of 4.1 ± 1.0 mm/yr (Villamor and Berryman 2006). The subsidence rates in both grabens are significant for evaluating the climatic and volcanic evolution in the southern TVZ because, if maintained over the lifetimes of the volcanoes, the original bases of the volcanoes will have been down-faulted (and buried) by hundreds of metres during their eruptive histories.

The mountains and ring-plain

The volcanoes of the TNP area take a variety of forms, including some smaller cones, but are dominated by the large stratovolcanoes of Ruapehu and Tongariro, which are surrounded by extensive ring plains consisting of volcaniclastic products and eroded volcanic material. Several younger satellite cones and craters, comprise lavas and pyroclastics forming Pukeonake at Tongariro (Beier et al. 2017), Saddle Cone and Ohakune Craters at Ruapehu (Houghton and Hackett 1984; Kósik et al. 2016), and a small vent east of Ruapehu close to the Desert Road named Te Roro o Taitearikī (named here, for the important place-name at this location; Ngāti Rangi/J Robinson pers comm, 2020).

Evolution and geochronology

The oldest rocks dated at Tongariro are 512 ± 59 ka. They represent a previous, independent edifice now almost entirely buried beneath the NW flanks of Tongariro (Pure et al. 2020). Volcanism at Tongariro itself began at ~350 ka (Pure et al. 2020). Combined with published K/Ar age data (Hobden et al. 1996), $^{40}Ar/^{39}Ar$ dating of Tongariro lavas (Pure et al. 2020) indicates building of the present edifice had definitely begun by ~230 ka (Figure 6). Townsend et al. (2017) subdivided Tongariro eruptives into thirteen formations (Figure 7) that have now been refined to ten by Pure et al. (2020) and subdivided into thirty six members that represent distinct phases of edifice growth and/or effusive pulses from individual vents across Tongariro.

In contrast, the oldest dated rocks of the Ruapehu edifice are only ~200 ka (Gamble et al. 2003). Eruptive products are divided into four main formations (Figure 7) at Ruapehu (Hackett and Houghton 1989; Figure 8) representing sequential phases of edifice

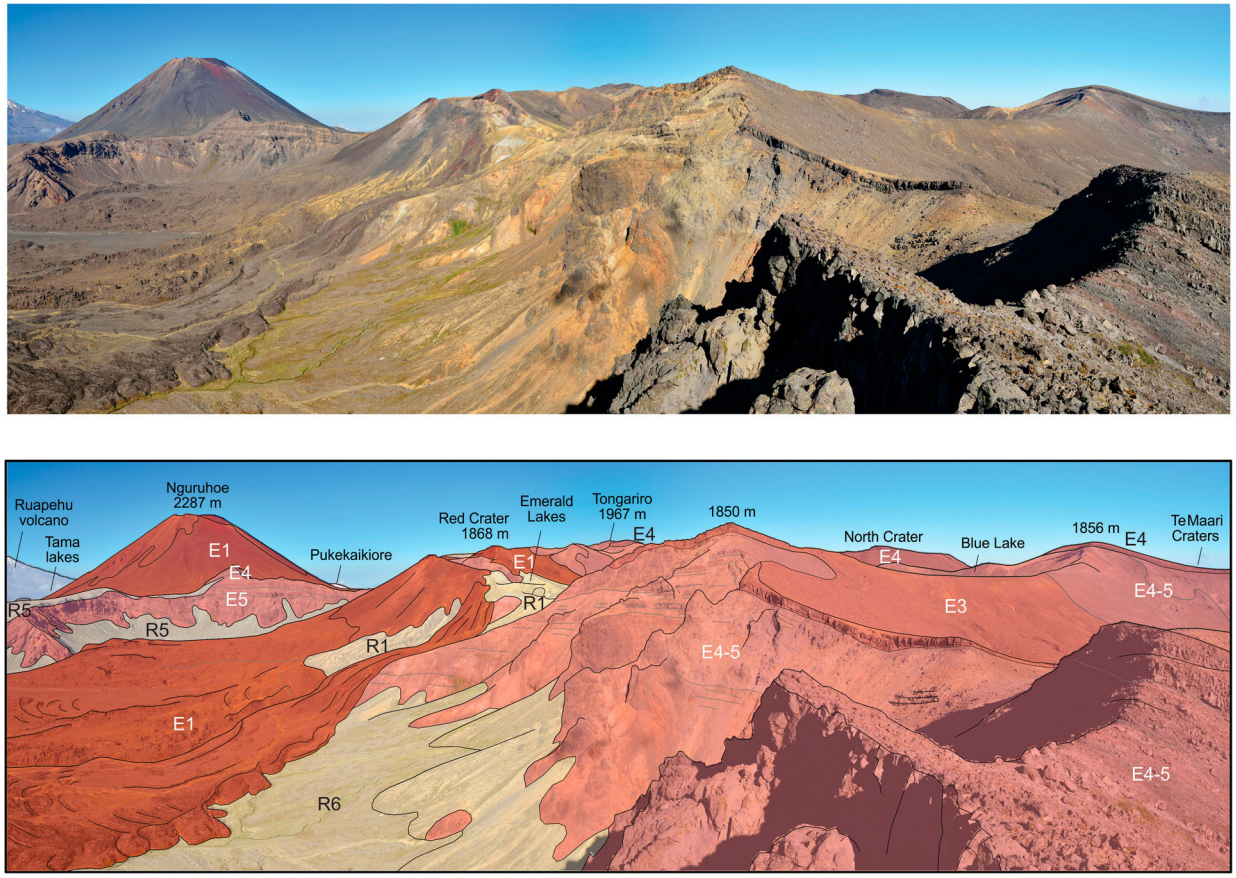

Figure 6. View looking southwest across Tongariro showing the relationship of ice-bounded lavas and breccia confined to high topography, and younger draping lavas and pyroclastic deposits that descend into the valley floors. Note also the symmetrical Ngāuruhoe cone, emplaced in a relatively ice-free environment. See Figure 3 for key to rocks labelled in the lower panel. Modified from Pure et al. (2020).

growth: Te Herenga (200–150 ka); Wahianoa (166–80 ka); Mangawhero (50–15 ka) and Whakapapa (<15 ka) (Gamble et al. 2003; Conway et al. 2016). The Mangawhero and Whakapapa formations have been subdivided into nineteen members based on their ages and geochemical compositions (Conway et al. 2016; Townsend et al. 2017). Dating of lava flows, where possible, has been integrated with cosmogenic dating of intercalated moraines (Eaves et al. 2016a). Further refinement of some late Holocene eruption ages has been achieved by correlating palaeomagnetic data with sediment secular variation records (Greve et al. 2016). Palaeomagnetic data also show that some Mangawhero Formation lavas captured the ~41 ka Laschamp geomagnetic excursion, placing tight constraints on their ages (Ingham et al. 2017).

Edifice geology and volcano-ice interaction

The TNP mountains are dominantly composed of lava (with autobreccia), intercalated with till and minor pyroclastic deposits (Hackett and Houghton 1989). The eruptive histories of the current edifices have coincided with several glacial-interglacial cycles, with summit ice caps and valley glaciers advancing during the glacial periods (Eaves et al. 2016b). Volcano building continued alongside glacial ice (Figure 9A–C), such that both volcanoes grew in a 'starfish' fashion, whereby lava accumulated along ridges (key ridge and flank growth periods denoted in Figure 7) and was largely excluded from valleys by glaciers (Conway et al. 2015; Townsend et al. 2017; Cole et al. 2018; Pure et al. 2020). This scenario contrasts with traditional models of edifice building in which symmetrical cones are formed and then incised by periods of glacial erosion (e.g. Singer et al. 1997). Lava that was impounded by ice shows characteristic chilling and jointing patterns (Spörli and Rowland 2006; Conway et al. 2015), while any eruptives emplaced over the ice were lost to the ring plain as debris. At Tongariro and Ruapehu, variations in edifice growth rates are similar, even though the volumes were calculated using different methods (cf. Conway et al 2016; Pure et al 2020). At Tongariro in particular, growth rates during glacial periods Marine Isotope Stage (MIS) 6 and 4–2 were only ~20% of those in interglacial periods MIS 5 and 1, likely due to conveyance of supra-glacial eruptive materials to the ring-plain in the glacial periods (Figure 10A,B).

Glaciovolcanic products, particularly ice-confined lavas, and glacial features such as moraines are ubiquitous on Ruapehu (Figure 9A–C; Conway et al. 2015).

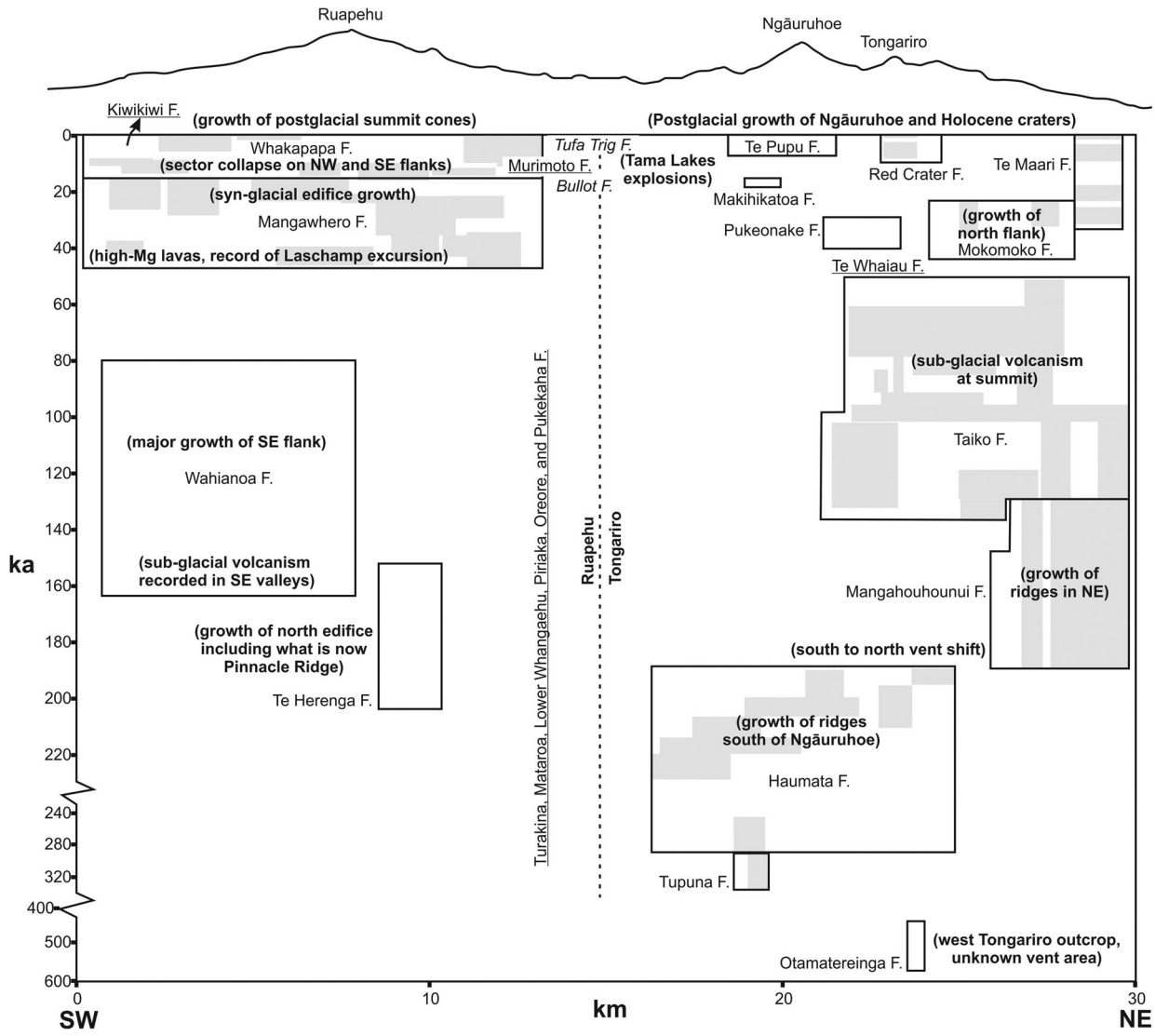

Figure 7. Volcanic formations of Ruapehu and Tongariro illustrated in time and in space from southwest to northeast. Black boxes enclose labelled primary volcanic formations (F). Grey boxes represent constituent members of those formations (see Townsend et al. 2017 and Pure et al. 2020 for details of those members). Airfall tephra formations named in text in italics. Volcaniclastic formations named in text underlined. Major events in the formation of these volcanoes are annotated in bold in parentheses. Growth of ridges is interpreted to represent emplacement of ice-lateral stacks of volcanic rocks forming planezes between glaciers (e.g. Conway et al. 2015). The reader is referred to Townsend et al. (2017, Figure 72) for a series of time slice cartoons depicting this evolution.

Breccias and ice-confined lavas in the Te Herenga and Wahianoa formations indicate subglacial and ice-marginal emplacement of eruptive products during the penultimate glacial period (MIS 6; Conway et al. 2016; Townsend et al. 2017; Cole et al. 2020). More extensive ice-confined lavas dominate the volcanic products of the Mangawhero Formation. $^{40}Ar/^{39}Ar$ ages for these lavas, along with their distribution and morphologies, indicate that valley glaciers descended to ~1300 m above sea level between 51–41 and 27–15 ka (MIS 2 and 3: Spörli and Rowland 2006; Conway et al. 2015; Eaves et al. 2016a, 2016b; Townsend et al. 2017). Subaerial valley-floor lava flows characterise the Whakapapa Formation and indicate that glaciers began to retreat at about 15 ka.

Moraines are also preserved extensively on Tongariro, indicating that glaciers filled valleys during the glacial periods MIS 6 and 4–2 (Eaves et al. 2016a, 2016b; Pure et al. 2020). Additionally, valley glaciers up to 250 m thick are inferred to have been present from thickened, valley-marginal lava flows emplaced around the end of MIS 7 and the transition to MIS 6 (Pure et al. 2020). Subaqueously-emplaced volcaniclastic deposits intercalated with ice-confined lavas are also exposed around the summit area of Tongariro, indicating eruption into an ice cap/summit glacier during the MIS 5–4 transition (Figure 9C; Cole et al. 2018).

The absence of ice has allowed symmetrical volcanic cones to form, such as North Crater and Ngāuruhoe (in the Holocene) on Tongariro. The early Holocene cones at Ruapehu, however, were still impounded to some degree by ice (Townsend et al. 2017). In general, glaciovolcanic interaction is less

Figure 8. Relationships between ice-bounded lava flows confined to high topography, moraine-bounded glacial valleys, and post-glacial lava flows in-filling valleys on the north-western flank of Ruapehu (modified from Conway et al. 2015). Aerial photograph (upper panel) and draped simplified geology (lower panel; see Figure 3 for legend). The snowline is at about 1700m elevation in this image. GNS Science photo by Dougal Townsend

apparent at Tongariro compared with Ruapehu. A relationship between subsidence due to rifting, edifice elevation and ice accumulation is likely to exist. Tongariro is lower in elevation and its vents are more dispersed along the rift, which may be a consequence of a longer-lived magmatic system at Tongariro, and/or distributed deformation due to rift faulting; it is transected by many normal faults (Gómez-Vasconcelos et al. 2017; Pure et al. 2020). Ruapehu, on the other hand, has only two closely-spaced primary vent loci (Conway et al. 2016; Townsend et al. 2017). The more extensive glaciation at Ruapehu may be a consequence of it growing taller and having a rain shadow effect on Tongariro, and/or loss of snow accumulation potential at Tongariro through a decrease in elevation by rifting (Eaves et al. 2016b; Pure et al. 2020).

Ring-plains: pyroclastic, lahar and sector-collapse deposits

As well as effusive activity, which has dominantly built the edifices, the TNP volcanoes have also undergone periods of heightened explosive activity, leading to the deposition of andesitic tephras intercalated with fluvial and laharic deposits on the ring-plains. Edifice versus ring-plain volumes, in cubic kilometres, are about 150:150 for Ruapehu (Conway et al. 2016)

Figure 9. Examples of eruptive materials comprising the edifices and ring plains. **A:** Tabular ice-marginal lava flows exposed in the Whangaehu valley wall, Ruapehu, inferred to have been confined against a retreating Whangaehu Glacier. Some flows have quenched glassy knuckles and lobes (k), where the lava excavated cavities in the glacier margin, and they overlie or intrude till (t). The lava (wim) that forms the c. 30 m high waterfall is interpreted to have been emplaced subglacially in a meltwater tunnel when the Whangaehu Glacier occupied this gorge, creating an internal mould of the tunnel. The rubbly lava flow (wc) is from Te Wai ā-Moe/Crater Lake and was deflected from entering the gorge by the glacier, instead deviating along the higher margin of the gorge to the left of the photo. GNS Science photo by Dougal Townsend; **B:** Characteristic cooling fractures orientated perpendicular to the margin of ice-bound lava, formed by quenching when the lava contacted ice. Photo by Colin Wilson; **C:** Bedded lapilli tuff deposits bearing fluidal bombs with quenched rinds. Bombs (b) are aligned parallel to bedding and their basal surfaces scour the underlying bedding, rather than form impact sag structures. The bombs are ~ 30 cm in diameter. Bedding is lenticular (lb) and defined by grain size variations with individual beds well sorted. Traction structures indicate emplacement from water along the steep summit ridgeline of Tongariro volcano. The lapilli tuffs are interpreted as subaqueous density current deposits emplaced in meltwater channels confined by a summit ice cap. Photo by Rosie Cole. **D:** Airfall ash and lapilli aged between c. 25 and 12 ka mantle blocky distal lava flows (to the left) from Ruapehu volcano near the Desert Road. The bank of tephra at right is about 3 m high. GNS Science photo by Dougal Townsend.

and 90:60 for Tongariro (Pure et al. 2020). Tephra carried further afield on the prevailing westerly winds has been preferentially deposited to the east and northeast of both volcanoes (Figure 9D; Topping 1973).

Radiocarbon-dated rhyolitic tephra layers (Wilson 1993; Vandergoes et al. 2013), mainly from Taupo volcano, provide age constraints for the andesitic tephra beds and intercalated deposits on the ring plains (Donoghue et al. 1995a; Cronin et al. 1996a). A complex tephra record extending to >70 ka is exposed on the eastern ring plain (Donoghue et al. 1995a; Cronin et al. 1996a, 1997a). Ruapehu contributed the most pyroclastic material between 25.5 and 11 ka (Bullot Formation, a non-mapped airfall tephra formation: Donoghue et al. 1995a). Analysis of Ruapehu tephra deposits from ~25.5 to 11 ka BP shows a change at around 13.5 ka from eruptions with steady plinian columns, to eruptions producing pyroclastic density currents from unsteady columns (Pardo et al. 2012a, 2012b, 2014; Cowlyn 2016). There was an intense ~200-year-long period of large explosive eruptions around 11 ka from multiple vents between Tongariro and Ruapehu (Pahoka-Mangamate sequence; Nakagawa et al. 1998; Auer et al. 2015, 2016) that has been linked to rupturing of regional-scale faults and accelerated rifting (Nairn et al. 1998; Heinrich et al.

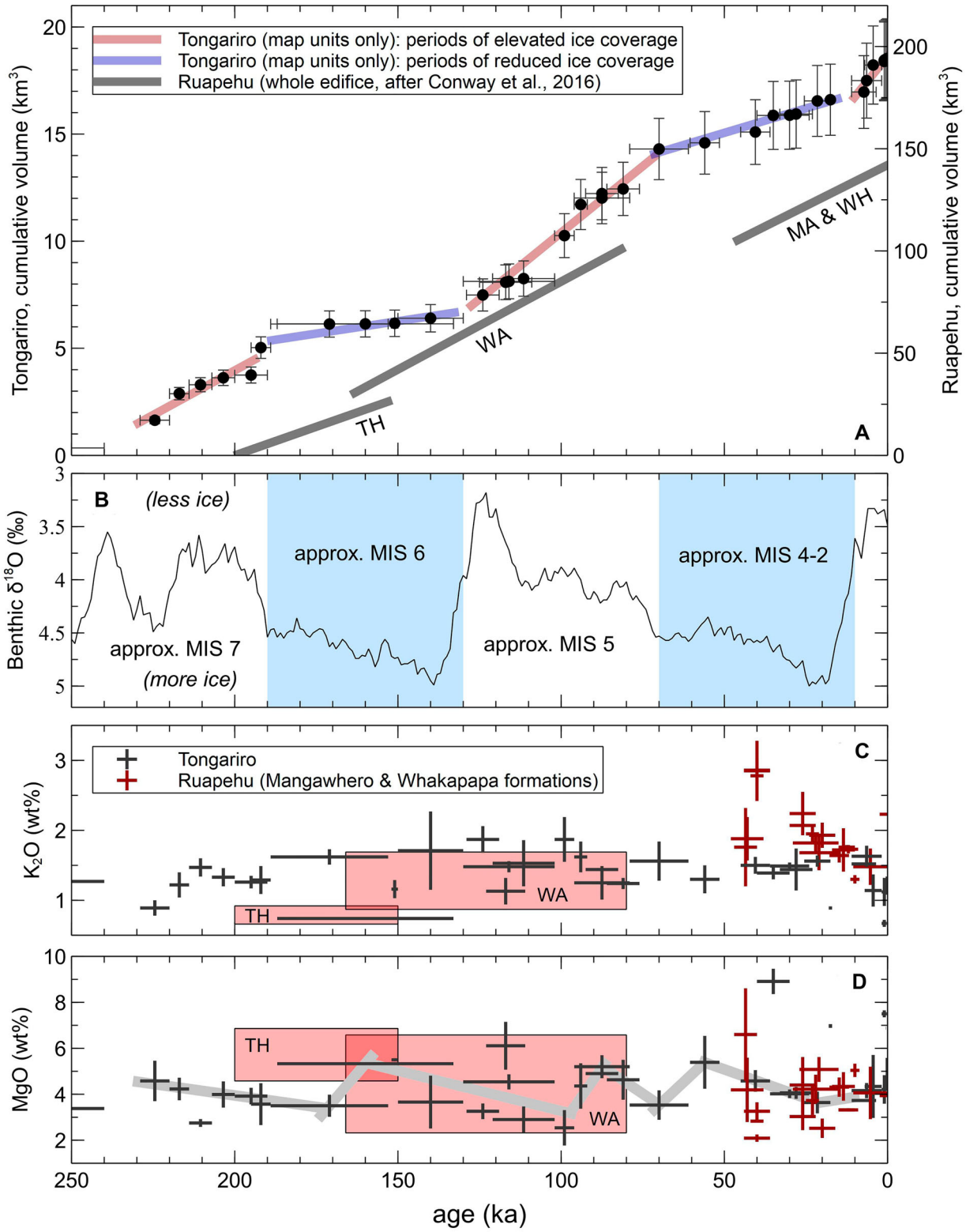

Figure 10. Summary of time, volume and composition variations of mapped units at Ruapehu and Tongariro volcanoes based on radiometric dating by Gamble et al. (2003) and Conway et al. (2016) for Ruapehu, and Pure et al. (2020) for Tongariro. **A**: Cumulative erupted volumes of Tongariro map units (left axis) and Ruapehu's total edifice (right axis), adapted from Pure et al. (2020) and Conway et al. (2016), respectively. For Ruapehu: TH: Te Herenga Formation, WA: Wahianoa Formation, MA: Mangawhero Formation, WH: Whakapapa Formation. **B**: Benthic $\delta^{18}O$ global climate proxy record from Lisiecki and Raymo (2005) with approximate positions of Marine Isotope Stage (MIS) periods shown. Blue shading indicates periods of valley-filling glaciers and ephemeral summit ice caps on Tongariro and Ruapehu as inferred by field geology (Conway et al. 2016; Townsend et al. 2017; Cole et al. 2018, 2019; Pure et al. 2020). **C**: Chronological variations in K_2O for Tongariro (dark crosses) and Ruapehu (red boxes and crosses). Cross heights show the variation in sample concentrations for each map unit; cross widths show minimum and maximum possible age range for each map unit. Ruapehu data from Gamble et al. (2003), Conway et al. (2016, 2018), and Tongariro data from Hobden et al. (1996), Townsend et al. (2017) and Pure et al. (2020). **D**: As for 'C' but for MgO. Thick grey lines show regressions between Tongariro data points as presented in Pure et al. (2020).

2020a). There is evidence for faster rifting of the Tongariro Graben propagating from north to south during this roughly 200 year period (Heinrich et al. 2020a). Gómez-Vasconcelos et al. (2020), however, found that movement on the Waihi and Poutu faults was at low levels during this period.

After 10 ka, explosive eruptions dropped in intensity and volume by an order of magnitude, and a period of relative explosive inactivity began at Ruapehu. Many tephras, mainly sourced from Tongariro, were deposited from 12 to 2.5 ka, and from Ngāuruhoe between 2,500 and 1,800 years ago (Topping 1973; Donoghue et al. 1995a; Moebis et al. 2011; Heinrich et al. 2020a). Volcaniclastic deposits (Kiwikiwi Formation) in the middle Whangaehu valley on Ruapehu reflect a late Holocene intense but only weakly-explosive eruption sequence through Te Wai ā-Moe/Crater Lake (Auer et al. 2012), or perhaps as an initial phase of building the cone that the lake now occupies. The Kiwikiwi formation overlies the 5 ka deposits of the Mangaio Formation in the Whangaehu Valley (Graettinger et al. 2010). The latter resulted from the inferred sector collapse of a hydrothermally altered cone, interpreted to be a predecessor to the modern cone hosting the lake (Townsend et al. 2017). Most recently, the Tufa Trig Formation (a non-mapped airfall tephra formation from Ruapehu) includes ashfall deposits from multiple eruptions younger than the 1,800 years ago Taupo ignimbrite from Taupo, through to present. Deposits of the Tufa Trig Formation are preserved in places throughout approximately the northern half of the TNP area and comprise at least nineteen andesitic tephras, each representing a moderate explosive eruption (one every ~100 years, on average) through Te Wai ā-Moe/Crater Lake (Figure 9D; Donoghue et al. 1997). Voloschina et al. (2020) add further detail to the Tufa Trig Formation sequence and explore the complexity of these eruptions. Preservation bias favours the identification of large tephra eruptions over small ones at TNP (as demonstrated in the work of Voloschina et al. 2020). Moebis et al. (2011) have shown, however, that the sources of thin and fine layers of tephra that are preserved on and near the volcanoes may be distinguished by the major element geochemistry of the glassy groundmass.

The extensive ring-plains surrounding Tongariro and Ruapehu have been largely built up from eruptive products that were transported away by lahars (Figure 3). Cronin and Neall (1997) identified fifteen lahar sedimentation 'episodes' in the north-eastern sector of the Ruapehu ring-plain, and five on the eastern Tongariro ring-plain. Further subdivision of Ruapehu ring-plain deposits has been achieved in the west (Lecointre et al. 1998) and south (Donoghue and Neall 2001). During glacial times, an increase in physical weathering (Cronin et al. 1996a; Cronin and Neall 1997) and conveyance of volcanic products deposited on to ice likely contributed to an increased sediment supply (Pure et al. 2020). On a more recent and smaller scale, lahars were generated by explosive eruptions involving expulsion of water from Te Wai ā-Moe/Crater Lake and entrainment of snow during the 1995 and 2007 eruptions at Ruapehu (Cronin et al. 1996b; Lube et al. 2009; Kilgour et al. 2010).

Sector collapses of high stratovolcanoes feed debris avalanches (Mount St Helens 1980 being the most spectacular modern example: Voight et al. 1983) and are another mechanism by which volcanic edifices become eroded and ring-plains grow. Debris avalanches may also transform with increasing run-out distances into debris flows and flood flows. Debris avalanches are known to have occurred on both volcanoes, with the most evident products being the 50–45 ka Te Whaiau Formation (Lecointre et al. 2002; Pure et al. 2020) on Tongariro and the 10.6 ka Murimotu Formation (Figure 11; Palmer and Neall 1989; McClelland and Erwin 2003; Eaves et al. 2015) on Ruapehu (i.e. the Whakapapa 'mounds'). Debris flows from other events (e.g. Donoghue and Neall 2001; Tost and Cronin 2015, 2016) were channelled for long distances downstream in several catchments and are incorporated into ring-plain deposits, including those of the Hautapu, Mangawhero, Whakapapa and Whangaehu rivers. The 349–309 ka Turakina Formation distal runout deposits extend >100 km downstream from TNP, and it is unclear whether they were sourced from Tongariro or Ruapehu. Radiometrically-determined ages of the clasts and clast petrographies are more indicative of a Tongariro source (Pure et al. 2020).

Ruapehu structure from geophysical data

A three-dimensional seismic tomography model (Rowlands et al. 2005) shows a reduction in *P*-wave velocity beneath the eastern flank of Ruapehu from 3 to 7 km depth (Figures 5 and 12A). Several explanations were put forward including hydrothermal alteration, partially molten material remaining from the 1995–96 eruption, downwarping of the crust by the load of the edifice, and thick deposits of pyroclastic and laharic material. The resolution is too poor, however, to favour any one interpretation. Seismic ambient noise cross correlation shows gradual increases in shear wave velocity at a rate of ~0.2 km/s per km depth beneath Ruapehu, interpreted to suggest that velocity increases from compaction are offset by progressive hydrothermal alteration (Godfrey et al. 2017).

One-dimensional inversion of MT soundings at Ruapehu (Ingham et al. 2009) shows a high resistivity layer at the surface that is a few hundred metres thick, above a lower resistivity layer, which in turn rests on higher resistivity material interpreted as greywacke

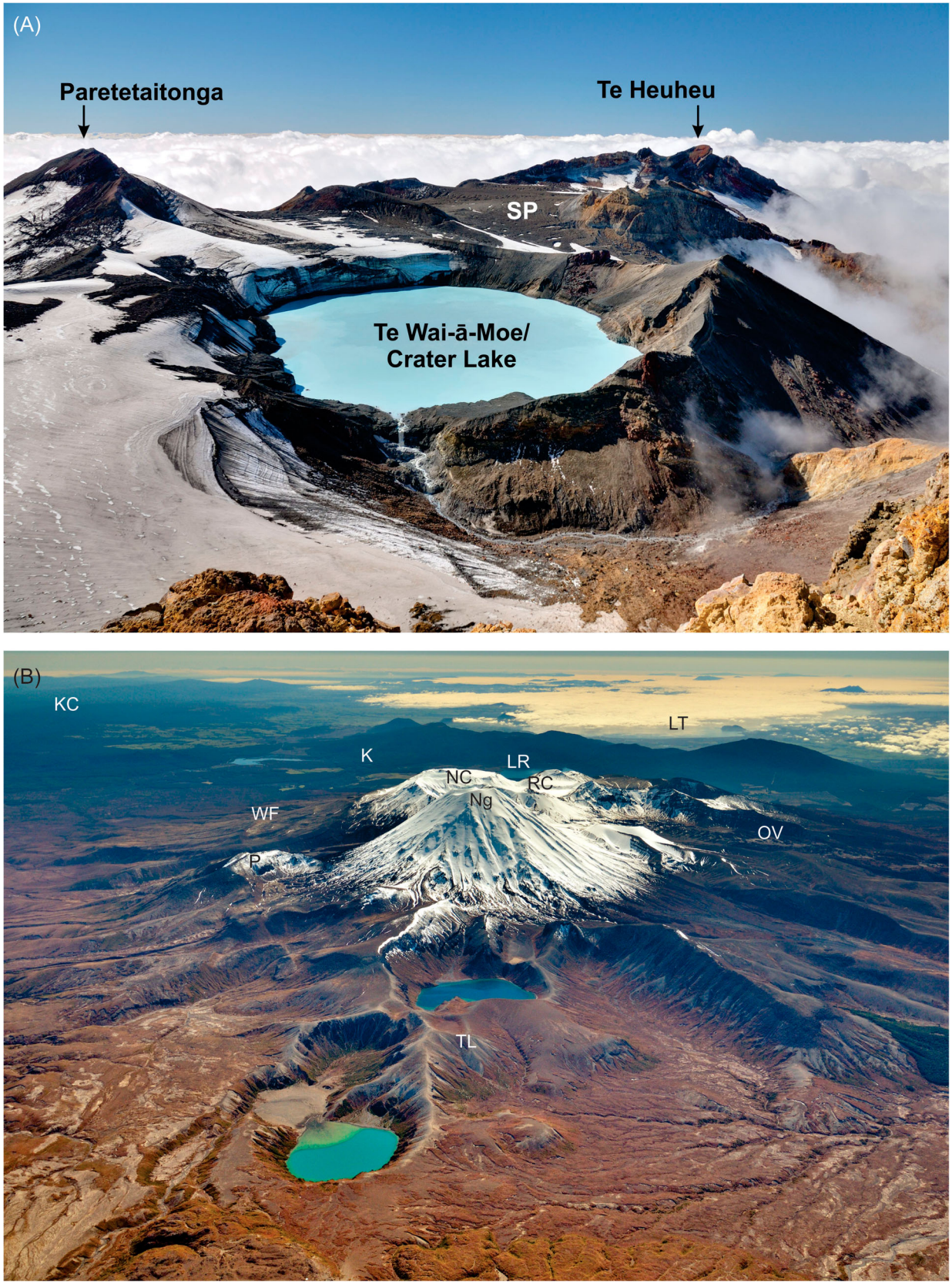

Figure 11. A: View of Ruapehu's Summit Plateau (SP) and Te Wai-ā-Moe/Crater Lake looking north, modified from Townsend et al. (2017). The collapse of a cone that had formed on the northern summit prior to the Holocene (between the Paretetaitonga and Te Heuheu peaks) led to the Murimoto Formation debris avalanche (Figure 1) near Whakapapa, possibly as further ice loss debuttressed its support. That scarp was then filled in with the early Holocene cone beneath the Summit Plateau. A similar process in the lead up to the Holocene occurred with the building of a cone in the foreground, which then collapsed to the right (eastward). The scar then filled in with a cone, the crater of which is now occupied by Te Wai ā-Moe/Crater Lake. **B**: View of Tongariro looking north, including the older, eroded Tama Lakes (TL) area lavas and Pukekaikiore (P) cone, and the Holocene cones and vents of Ngāuruhoe (Ng), North Crater (NC), Red Crater (RC). Lakes Rotoaira (LR) and Taupo (LT) are to the north, and Oturere valley (OV) trends east from the high peaks of the Tongariro edifice. The King Country (KC) lies to the west.

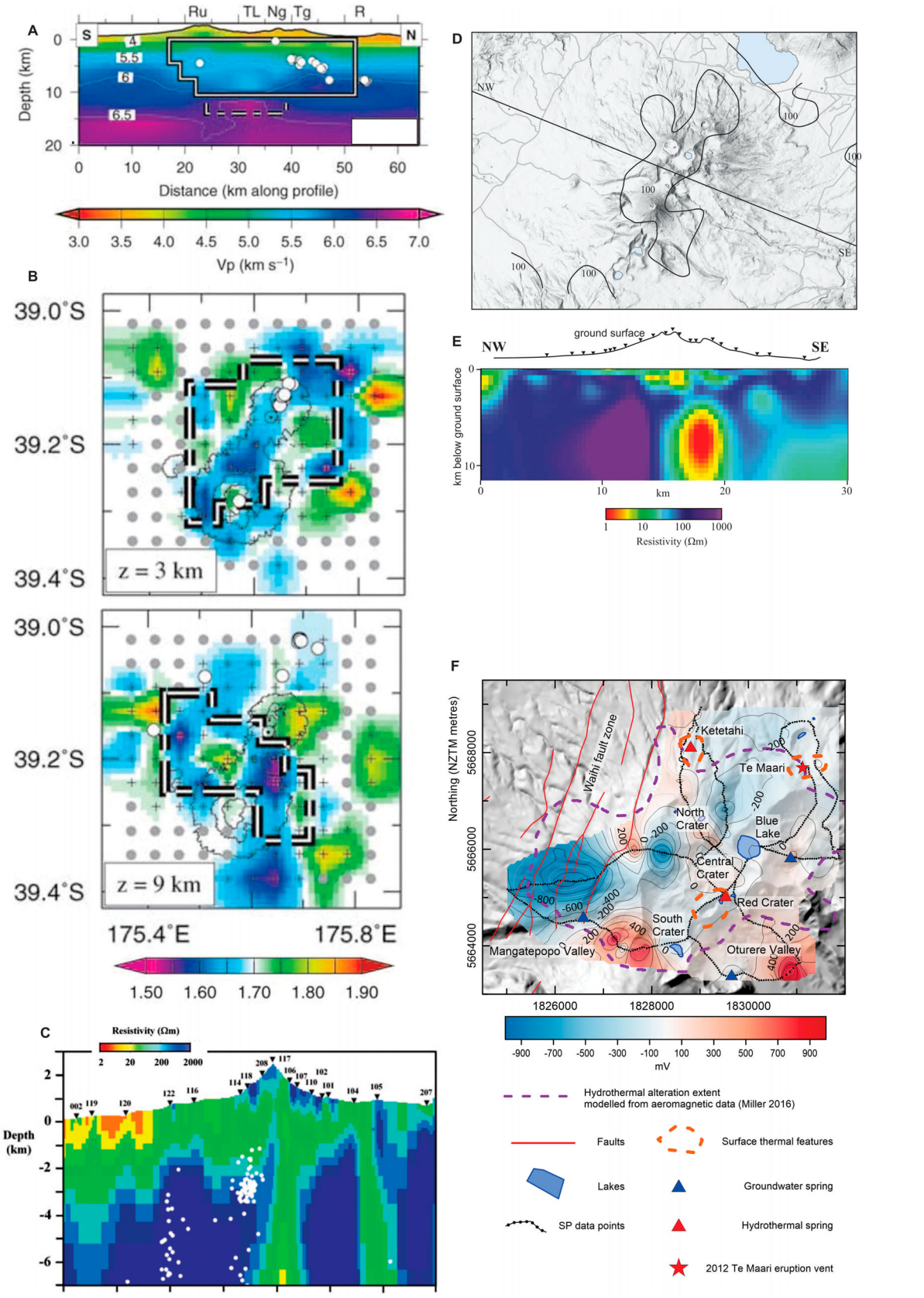

Figure 12. Geophysical data from Ruapehu and Tongariro. **A**: V_p data beneath Ruapehu and Tongariro (top). **B**: V_p/V_s ratios at 3 (upper) and 9 km (lower) depth beneath Tongariro. A and B reproduced as authorised by the publisher from Figures 8 and 10 of Rowlands et al. (2005). **C**: 2D resistivity model beneath Ruapehu reproduced as authorised by the publisher from Figure 9 of Ingham et al. (2009). Note that this is a 2-D inversion of a single line of data over Mount Ruapehu, much less reliable than a 3-D inversion. **D** and **E**: resistivity in plan (at 2.5 km depth) and section view of 3D MT model at Tongariro (modified from Hill et al. 2015). The closed 100 ohm-m contour in 'D' indicates the approximate extent of hydrothermal alternation. **F**: Self-potential anomalies at Tongariro (modified from Miller et al. 2018a). Self-potential data points are shown by the black dotted line. The purple dashed line outlines the extent of hydrothermal alteration from magnetic data and the orange dashed line outlines surface thermal features. Red and blue triangles are hydrothermal and groundwater springs, respectively, and the red star indicates the 2012 eruption vent.

basement (Figure 12B). The high resistivity surface layer is interpreted as unaltered surface volcanic rocks, consistent with high magnetic susceptibility areas imaged by 3D aeromagnetic inversion (Miller et al. 2020). The low resistivity layer is interpreted to be the hydraulically controlled upper limit of a zone of hydrothermal alteration. South and west of Ruapehu, deeper low resistivity layers correspond to the Tertiary sediments.

Three-dimensional inversion of MT data shows a vertical, low resistivity sheet-like feature extending to at least 10 km depth to the northeast from beneath the summit of Ruapehu. This feature is also consistent with a lack of seismicity east of the summit, supporting the interpretation that this conductive zone is a conduit for hot fluids, although Ingham et al. (2009) considered it unlikely that this zone reflects the presence of magma. However, the depth of the conductor is consistent with the depths of magma storage derived from volatile contents of phenocryst-hosted melt inclusions of 2–9 km (Kilgour et al. 2013), so a magmatic source cannot be completely ruled out. The location of the low resistivity sheet-like feature is broadly similar to the low V_p anomaly reported by Rowlands et al. (2005). The combined geophysical and petrological evidence suggest that the conductor and low V_p zone may be evidence for a vertically extensive magma storage system supplying Ruapehu.

Other MT studies of Ruapehu's Summit Plateau (Jones et al. 2008), show a shallow broad, low-resistivity zone underlying the entire plateau, which is interpreted to represent hydrothermally altered rock. Within this low-resistivity zone, and beneath the northern and central parts of the plateau, there are two localised more resistive regions. These are inferred to be dominated by chlorite alteration, indicating higher temperatures and the existence of relict heat pipe systems from when the active vent was to the north of the modern Te Wai ā-Moe/Crater Lake (Jones et al. 2008). The shallow conductive layer is also coincident with material of generally low magnetic susceptibility beneath the summit plateau, consistent with the inference of hydrothermal alteration (Miller et al. 2020).

Inverse models of aeromagnetic data, combined with analysis of hyperspectral images of Mt Ruapehu (Miller et al. 2020; Kereszturi et al. 2020) show large areas of low magnetic susceptibility and of clay minerals, interpreted as the products of hydrothermal alteration, on the southeastern flank of the edifice and affecting rocks of the Wahianoa Formation (Figure 4B). A high magnetic susceptibility body beneath the southern side of the Whangaehu valley is modelled as a sill and may have been fed by dikes now visible in the valley walls. A thick sequence of high magnetic susceptibility material, interpreted as buried ~150–50 ka lavas, is imaged beneath the northern flanks of the mountain (Figure 4B). High magnetic susceptibility bodies are interpreted as unaltered dykes intruding the otherwise variably altered Te Herenga Formation exposed at Pinnacle Ridge. Comparison of aeromagnetic data from Ruapehu and Tongariro (e.g. Miller and Williams-Jones 2016) shows that hydrothermal alteration is more fragmentary across the whole edifice of Ruapehu compared to Tongariro. This may reflect the more focussed vent systems feeding long-lived volcanism at Ruapehu, which concentrates hydrothermal activity at discrete locations for long periods of time; compared with the long-term widely-distributed nature of volcanism at Tongariro, which has resulted in a broader widespread alteration footprint.

Tongariro structure from geophysical data

A shallow low V_p anomaly lies beneath Tongariro volcano, coincident with a large demagnetised, low-density area to the north of Ngāuruhoe as revealed by aeromagnetic and gravity surveys, and a shallow low resistivity zone modelled from MT data (Figures 4A and 12A, B; Rowlands et al. 2005; Hill et al. 2015; Miller and Williams-Jones 2016). These features are most likely to be related to the active, vapour-dominated geothermal field and resulting hydrothermal alteration (Figures 5 and 12C; Miller et al. 2018a). The demagnetised area, inferred to indicate the extent of Tongariro's hydrothermal system, is bounded by the major rift faults to the east and west, which act to impede fluid movement (Miller and Williams-Jones 2016).

MT imaging also reveals a vertically extensive zone of lower resistivity extending from beneath Ngāuruhoe to Te Maari at 4–12 km depth (Figure 12). This zone is comparable in resistivity and depth extent to that seen in 3D inversions of MT data to the east of Mt Ruapehu (Ingham et al. 2009), but is better constrained by measurements than the anomaly at Ruapehu (see above). The deep Tongariro anomaly is interpreted as a connected crustal magma storage zone (Figure 5; Hill et al. 2015). Linking the hydrothermal system and magma storage zone is a zone of slightly higher resistivity interpreted as a pathway of altered or porous rock that enables aqueous fluids to ascend from depth to the surface (Hill et al. 2015). This is similar to the interpretation by Ingham et al. (2009) for the deep conductive Ruapehu anomaly, as being a conduit whereby hot aqueous fluids are transported towards the surface. Seismic ambient noise cross-correlation at Tongariro shows greater shear wave velocity increases with depth compared with Ruapehu. These increases are interpreted to represent multiple zones within the rocks hosting the volcanic plumbing system above the basement greywacke (Godfrey et al. 2017).

A low V_p anomaly beneath Ngāuruhoe extends from 3 to 8 km depth (Rowlands et al. 2005). Ngāuruhoe is Holocene in age, which is too recent for any significant downwarping of the crust to have occurred. Remnant partial melt from recent eruptions stored in small, interconnected pockets is the most probable cause of this low-velocity volume, consistent with the wide geochemical variability of recent eruption products (Hobden et al. 1999; Rowlands et al. 2005). A magnetic high extending to the basement also coincides with a low-density zone beneath Ngāuruhoe and is interpreted as representing the unaltered conduit rocks (Figure 5; Miller and Williams-Jones 2016).

Magma systems

The andesites of Ruapehu and Tongariro have long been studied as typical products of arc stratovolcanoes (e.g. Clark 1960; Cole 1978; Graham and Hackett 1987). Major advances have since come from petrological studies incorporating isotopic and microanalytical techniques along with extended radiometric dating to establish edifice growth histories. New radiometric ages are from $^{40}Ar/^{39}Ar$ dating of devitrified lava groundmass samples (Gamble et al. 2003; Conway et al. 2016; Pure et al. 2020) and extend earlier whole-rock K/Ar data (Hobden et al. 1996). These data provide a precise chronostratigraphy within which magma evolution and andesite petrogenesis can be evaluated.

Petrological studies of TNP andesite lavas began with Clark (1960: initial petrographic descriptions, modal analyses) and Cole (1978: initial geochemical data) identifying these as typical plagioclase-pyroxene-phyric arc andesites. Subsequent stratigraphically controlled geochemical studies on Ruapehu were undertaken by Graham and Hackett (1987) confirming they are calc-alkaline andesites with a moderate K content. Price et al. (2012) and Conway et al. (2018) reconstructed Ruapehu's long-term compositional evolution. For Tongariro, Hobden (1997) provided the first detailed geochemical data coupled to radiometric dates (Hobden et al. 1996), with the most recent work by Pure (2020) and Pure et al. (2020) reconstructing the long-term compositional evolution of the volcano. Other papers have examined products of individual vents, particularly the Ngāuruhoe cone (Hobden et al. 1999, 2002; Price et al. 2010). In parallel with petrological work on lavas of all ages, numerous papers have dealt with the compositions of post-20 ka pyroclastic deposits from both volcanoes, although some focus on tephra correlation rather than petrological reconstruction. These are, for Ruapehu: Donoghue et al. (1995a, 2007), Gamble et al. (1999), Nakagawa et al. (1999, 2002), Auer et al. (2013), Kilgour et al. (2013, 2014) and for Tongariro: Nakagawa et al. (1998), Shane et al. (2008, 2017), Moebis et al. (2011), Auer et al. (2015) and Heinrich et al. (2020a). Of these young deposits, the most voluminous were erupted at around 11 ka and involved effectively synchronous eruptions from isolated magma bodies through aligned but distinct vents that span ~20 km across the Tongariro and Ruapehu systems (Nairn et al. 1998; Heinrich et al. 2020a).

Most rocks from both Ruapehu and Tongariro are porphyritic, with phenocryst contents of ~10–40% (in some cases more) and assemblages dominated by plagioclase, followed by subequal amounts of orthopyroxene and clinopyroxene, then lesser amounts of Fe-Ti oxides. Some rocks contain olivine and others more rarely contain apatite and amphibole. Groundmasses vary from cryptocrystalline to hypohyaline and, rarely, glassy. The combined 'cargo' of larger crystals includes phenocrysts and xenocrysts that show textural evidence for both equilibrium and disequilibrium processes, and carry melt inclusions of varied compositions: these characteristics are similar to those of arc andesites globally (e.g. Gill 1981). Xenoliths of crustal materials, millimetres to centimetres across, are ubiquitous and of either meta-sedimentary or meta-igneous origin (Graham 1987; Graham et al. 1988, 1990; Pure 2020).

Lavas from Ruapehu (Price et al. 2012; Conway et al. 2018) and Tongariro (Hobden 1997; Pure 2020) show similar compositional trends (Figure 13), but subtle differences. For example, the TAS diagram (Figure 13A; Le Bas et al. 1986) for Ruapehu and Tongariro show that samples range from basaltic-andesite to dacite and that Tongariro data are generally weighted towards more mafic compositions, whereas Ruapehu samples are generally more evolved. This contrast reflects differences in crustal processing (melting, crystallisation and zoning) and magmatic residence times at the two volcanoes. In the SiO_2 versus MgO plot (Figure 13C), the bulk of data from both volcanoes form an overlapping array, but a high-Mg suite, dominated by Ruapehu samples (Conway et al. 2018), runs subparallel to this array. Ruapehu high-Mg lavas were generated by influx of mantle-derived mafic magmas with entrained primitive olivines, which rapidly hybridised with mid-crustal felsic magma bodies prior to their eruption (Conway et al. 2020). Like TAS diagrams, K_2O versus SiO_2 data (Figure 13D) show overlapping Tongariro and Ruapehu arrays, but with Ruapehu samples extending to higher values. Sr-Nd-Pb isotopic compositions of Ruapehu and Tongariro eruptives provide clear evidence that magmas interacted with Mesozoic metasedimentary basement rocks, probably in the upper 15 km of the crust (Graham 1987; Hobden 1997; Harrison and White 2006; Price et al. 2010, 2012; Pure 2020). A notable distinction between pre- and post-150 ka lavas at Ruapehu volcano has been made on the basis of higher and lower $^{143}Nd/^{144}Nd$ values,

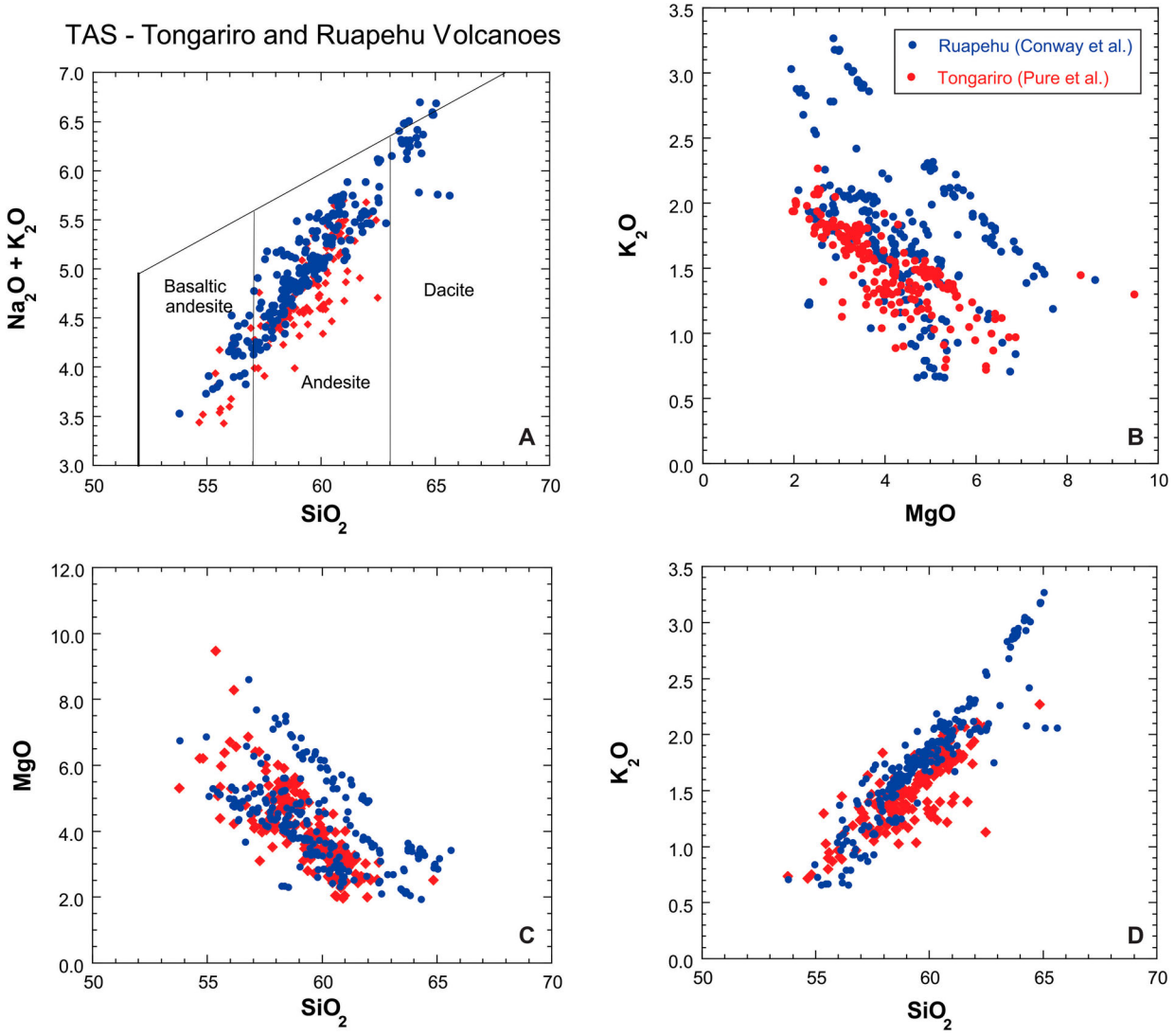

Figure 13. Representative figures to show compositional variations from mapped lavas on Ruapehu (blue) and Tongariro (red) volcanoes, based on data from Conway et al. (2016, 2018) and Pure et al. (2020). The plots are supplemented by published data from Hobden et al. (1997) for Tongariro, and Price et al. (2012) for Ruapehu. The TAS fields in panel **A**, defining basaltic andesite, andesite and dacite, are from Le Bas et al. (1986).

respectively (Price et al. 2005). This indicates that isotopically distinct crustal materials were assimilated in pre- versus post-150 ka magmas at Ruapehu, which may in turn reflect the development of a dispersed magma storage and plumbing system at a variety of crustal levels over time (Price et al. 2012). Available isotopic data do not show a comparable pattern at Tongariro (Hobden et al. 1996; Price et al. 2010; Pure 2020).

Although time-composition trends on decadal to millennial scales indicate individual magma batches were produced via complex and unique combinations of melting, mixing and fractionation (e.g. Gamble et al. 1999, 2003; Waight et al. 1999), compositional data for eruptive sequences at Ruapehu and Tongariro on longer time scales demonstrate systematic cyclic variations (Figure 10C, D). At Ruapehu, K_2O and MgO contemporaneously vary between 1–3 wt% and 2–8 wt%, respectively, showing excursions to more evolved then back to less evolved compositions from 50 to 0 ka (Conway et al. 2016). Time-MgO relationships for Tongariro reflect cyclic, volcano-wide mafic magma replenishment events, which occur over <10–20 kyr periods yielding MgO concentrations in erupted lavas of ~5–9 wt%, followed by decreases over 10–60 kyr to minima of ~2–4 wt% MgO. These variations may be linked to regional tectonic processes that regulate the connection between mantle-derived melts and multiple differentiating intra-crustal magmas (Figure 10D; Pure et al. 2020). Such cyclicity controls timeframes over which magmas with typical compositional ranges are produced in significant volumes (i.e. >10 km^3). Ruapehu displays a similar MgO cyclicity for high-resolution records from ~50 ka to present (Conway et al. 2018). At Tongariro these variations are uncorrelated with transitions between low and high rates of edifice growth (Figure 10D) and hence are independent of glacial-interglacial cycles (Pure et al. 2020).

Gamble et al. (1999), Hobden et al. (1999) and Nakagawa et al. (1999) show that the products of relatively small historic eruptions (<0.1 km^3) at Ruapehu and Tongariro are compositionally varied, reflecting independent sets of small magma sources of different compositions distributed through the crust beneath each volcano. At both volcanoes, small batches of melt are inferred to have been mixed or mingled and often have incorporated antecrysts from crystal mush zones traversed by the mixed melts (Donoghue et al. 1995b; Hobden et al. 2002; Nakagawa et al. 2002; Kilgour et al. 2013). Compositions of historic eruptive products (especially the 1995–96 Ruapehu eruptions: Gamble et al. 1999) thus show greater diversity than do those of larger edifice-forming eruptive sequences (>1 km^3) that accumulated over thousands to tens of thousands of years (Conway et al. 2018; Pure et al. 2020). This compositionally diverse but volumetrically minor activity, unlikely to be fully preserved in the geological record, probably represents 'background' activity that has persisted through the lifetimes of Tongariro and Ruapehu (Gamble et al. 1999).

Historic unrest and the hydrothermal systems

Volcanic activity in the last few thousand years in the TNP area has come from the single active vent of Ruapehu (Te Wai ā-Moe/Crater Lake), and from several vents on Tongariro, particularly Ngāuruhoe. Written historical records of these volcanoes date from the arrival of Europeans in the nineteenth century. These records, together with eruption information for a few preceding decades from Māori who arrived some six centuries earlier, are summarised in Gregg (1960) and Cole and Nairn (1975). Studies of historical eruptions at Ruapehu (Houghton et al. 1987; Scott 2013) and Tongariro (Figure 14; Scott and Potter 2014) considered the frequency of eruptive events and identified a high level of volcanic unrest and activity along with previously undocumented eruptions at Red Crater on Tongariro.

Geophysical signals and unrest

Ruapehu and Tongariro volcanoes often show signs of volcanic unrest, manifested as elevated gas fluxes, seismic activity, and lake and fumarole temperature and chemical changes. This unrest sometimes leads to periods of volcanic activity, ranging from weak hydrothermal (phreatic) through to phreatomagmatic and explosive magmatic activity, or may return to background levels (Park et al. 2019). Individual explosive eruptions sometimes occur with no precursors, or only a few minutes of precursory seismic activity. In a few cases lava extrusion also occurs (Ruapehu 1945, 1995; Ngāuruhoe 1870, 1949, 1954–5). The historic eruption hazards include pyroclastic density currents, ashfall, lava, debris avalanches, ballistic blocks and lahars: these are described in detail in the next section.

Seismic recording at Ruapehu started soon after the 1945 eruption, and it was soon found that harmonic tremor, a continuous waveform with a dominant frequency, usually about 2 Hz (as opposed to individual earthquake events), was often present, whether or not there was any obvious volcanic activity (Dibble 1974; Hurst and Sherburn 1993). Latter (1981) introduced the term volcanic earthquake to describe narrow-band earthquakes, also with a dominant frequency about 2 Hz. He described how strong volcanic earthquakes and large tremor amplitudes accompanied magmatic and phreatomagmatic eruptions, but there were many occasions in which similarly strong seismicity occurred without any eruption. These studies were extended by Bryan and Sherburn (1999) and Sherburn et al. (1999), who found that during the 1995–96 eruption sequence there were significant changes in the tremor pattern, with sub-1 Hz tremor accompanying presumed magmatic intrusions during an early stage of the 1995 eruption, while wideband tremor was dominant in the later part of the 1995 eruptions and in the 1996 eruption.

Earthquake swarms about 15 kilometres west of Ruapehu started some months before the 1995 eruption sequence and may have been precursory in some way as petrological studies have suggested that they coincided with the time of magma movement (Hurst and McGinty 1999; Hurst et al. 2018). Johnson and Savage (2012) confirmed that previous measurements of shear-wave splitting reliably detected changes in anisotropy, interpreted as being due to stress changes under Ruapehu around the time of the 1995 eruptions, but that using this technique to look for eruption precursors would be difficult because it would need the local seismicity distributed more evenly in time and space than is usually seen in the TNP area.

Latter (1981) also detected many volcanic earthquakes associated with eruptions at Ngāuruhoe until its most recent eruption in 1975, but since then there was a very low level of seismicity for many years. Between 2005 and 2010 there were thousands of very small (M_L < 1.8) earthquakes under Ngāuruhoe (Jolly et al. 2012; Park et al. 2019) but these have died away, and Ngāuruhoe remains inactive.

Tongariro has produced very little seismicity since seismometers were first installed near Ngāuruhoe in 1976, but small, slowly decaying earthquakes of the type known as tornillos were observed from 1999 for several years (Hagerty and Benites 2003), centred

Figure 14. View of Ngāuruhoe cone looking south across the Mangatepopo valley, with annotations of eruption products. Recent lava and pyroclastic deposits sourced from Ngauruhoe overlie older Tongariro lavas exposed in cliffs. GNS Science photo by Dougal Townsend.

below Te Maari craters on the north flank of Tongariro. No surface activity was observed at this time, but in late July 2012, there began several periods of shallow volcano-tectonic earthquakes up to M_L 2.8 in the same area (Hurst et al. 2014). It was also found that CO_2 emissions from Te Maari fumaroles had increased. At 11.46 pm NZST on 6 August 2012 a short-lived steam-driven eruption occurred, producing a 9 km high eruption column (Crouch et al. 2014). Analysis of seismic and acoustic records indicated that a debris avalanche had preceded and likely triggered the eruption (Jolly et al. 2014). A smaller eruption also occurred on 21 November 2012. There have been no further eruptions and the level of steam emission from the new vents has slowly decreased.

The use of geodetic measurements for detecting deformation on Ruapehu and Tongariro began with tilt and EDM measurements on Ruapehu in the 1970s by Ray Dibble and Peter Otway (unpublished). These measurements continued into the 1990s, but did not detect any significant precursory deformation to any of the eruptions that occurred in this period. In the early 2000s, a network of Global Navigation Satellite System (GNSS) stations was set up around the TNP volcanoes, but neither the September 2007 Ruapehu, nor the August 2012 Te Maari eruptions had detectable precursory deformation (Hamling et al. 2016). Hamling (2021) looked at the ability of satellite radar interferometry (InSAR), which has much better spatial resolution than GNSS, to detect precursory deformation, and concluded that it would be difficult to detect movements of small (<0.02 km^3, <340 m diameter sphere) magma bodies, although significantly larger ones would be reliably detected. Subsidence and gravity changes following the Te Maari eruption (Hamling et al. 2016; Miller et al. 2018b) show the adjustment of the hydrothermal system to depressurisation where liquid and vapour are redistributed within the hydrothermal system in response to changing pore pressures.

Hydrothermal systems

Ruapehu and Ngāuruhoe presently have only very minor hydrothermal activity away from their active craters, whereas the rest of Tongariro has a significant hydrothermal system with condensate outflows on its northern flank at Ketetahi (Figure 2; Wilson 1960), as well as the high-level hydrothermal features that feed the Emerald Lakes and Blue Lake areas (Walsh et al. 1998), and fumaroles at Te Maari. Miller et al. (2018a) used self-potential inversion to image the distribution of vapour and condensate within the hydrothermal system and proposed that the surface features are not part of a large continuous liquid

circulation system, but are discrete pockets of activity separated by regions of meteoric water downflow.

All the historic activity of Ruapehu volcano has been from the vent normally occupied by Te Wai ā-Moe/Crater Lake. The lake intercepts nearly all the heat output of the Ruapehu vent by condensation of incoming steam, and calorimetry of the lake can be used to monitor incoming heat (Hurst et al. 1991). The condensed steam is a considerable part of the inflow to the lake; however, precipitation and snowmelt, especially in summer, normally make a larger contribution. The lake temperature and level are telemetered daily by satellite, and GNS Science makes daily estimates of the thermal input power. The lake was completely expelled by the major eruptive sequences of 1945 and 1995, and was partially emptied by some of the smaller eruptions, but it has always eventually refilled, producing its own lahar hazard through overtopping of the outlet barrier (discussed below).

In addition to steam, the vapour entering the lake also carries magmatic volatiles which interact to varying degrees with the lake and sub-lake hydrothermal environments (Christenson 2000). Dissolution of SO_2, H_2S and HCl from this vapour leads to formation of a strongly acid lake water (Giggenbach 1974; Giggenbach and Glover 1975) that then convectively circulates through the sub-lake environment, interacting with host lavas, breccias and lake sediments as well as the incoming vapour (Christenson and Wood 1993). These interactions lead to the focussed deposition of a suite of hydrothermal minerals including elemental S, various sulphate minerals (principally natroalunite) and cristobalite, all of which drastically reduce permeability (Christenson et al. 2010).

An interesting characteristic of Ruapehu is that the heat and volatile supply to the lake is pulsatory, resulting in heating cycles where lake temperatures range between ~9 (minimum) and ~50 °C (maximum) over periods varying between 3 and 12 months. Analysis of solute gas compositions in the lake water began in 2007, and has produced time series trends that show that heating in the vent environment is coherent with lake heating, while CO/CO_2 equilibrium relations indicate model temperatures beneath the lake ranging from 400–750 °C.

A number of unheralded steam-driven eruptions have occurred since regular monitoring of the lake began in the early 1970s, some of which have occurred at times when the lake is cool (Strehlow et al. 2017), such as that on 25 September 2007. To explore this behaviour, a TOUGH2 model (Pruess 1991) of the lake/sub-lake environment was developed, with energy inputs constrained by observed parameters (Christenson et al. 2010). Modelling shows that vapour and heat inputs into the cool lake/vent environment lead to decoupling of heat and mass in the conduit, with the thermal front lagging behind an ascending, relatively cool and non-condensable CO_2-rich gas pulse. Accumulation of this gas beneath a relatively impermeable seal leads to the formation of a compressible gas column, capable of generating pressures greater than the tensile strength of the seal. This ultimately leads to seal failure and an unheralded, gas-driven eruption through the lake.

Historic volcanism, hazards and impacts

Ruapehu and Tongariro have erupted with a wide range of styles and associated hazards during their respective histories (e.g. Houghton et al. 1987). The most challenging eruptions in terms of assessing present-day hazards lie at the two ends of the historic size spectrum for TNP. (1) Small steam-driven eruptions (hydrothermal/phreatic to phreatomagmatic) are challenging because they occur with little or no warning, whereas (2) large magmatic explosive eruptions are challenging because they produce widespread hazards, the scales and durations of which are hard to forecast. The vent areas on both mountains are visited regularly by tourists (Tongariro Alpine Crossing, Ruapehu summit), putting people at risk from even small eruptions. Ashfall from larger eruptions could potentially affect most of the North Island, including impacts on major urban areas, depending on wind directions (Hitchcock and Cole 2007).

Notable historic eruptions have been: ash eruptions from Ruapehu in 1945, 1969, 1975 and 1995–96 (e.g. Gamble et al. 1999 and references therein; Cronin et al. 1997b, 2003; Bryan and Sherburn 1999; Bonadonna et al. 2005), lava eruptions from Ngāuruhoe in 1949 (e.g. Battey 1949) and 1954–55 (Figure 15; summary in Hobden et al. 2002), and ash-producing explosive eruptions from Ngāuruhoe in 1974 and 1975 (e.g. Nairn and Self 1978) and Te Maari on Tongariro in 1898 (Scott and Potter 2014). The latest eruption at Ruapehu with effects beyond Te Wai ā-Moe/Crater Lake was a steam-driven eruption in September 2007 (Cole et al. 2009; Kilgour et al. 2010; Jolly et al. 2010). The latest eruptions at Tongariro were a magmatic eruption of Ngāuruhoe in February 1975, and a steam-driven one at Te Maari in November 2012 (e.g. Jolly and Cronin 2014 and references therein).

Steam-driven eruptions

The recent Te Maari 2012 and Ruapehu 2007 eruptions have illustrated that even small steam-driven eruptions (where little or no magma reaches the surface) can produce multiple complex, interacting hazards, including ashfall, lahars, ballistics, pyroclastic density currents, and debris avalanches (Kilgour et al. 2010; Breard et al. 2014; Fitzgerald et al. 2014; Leonard

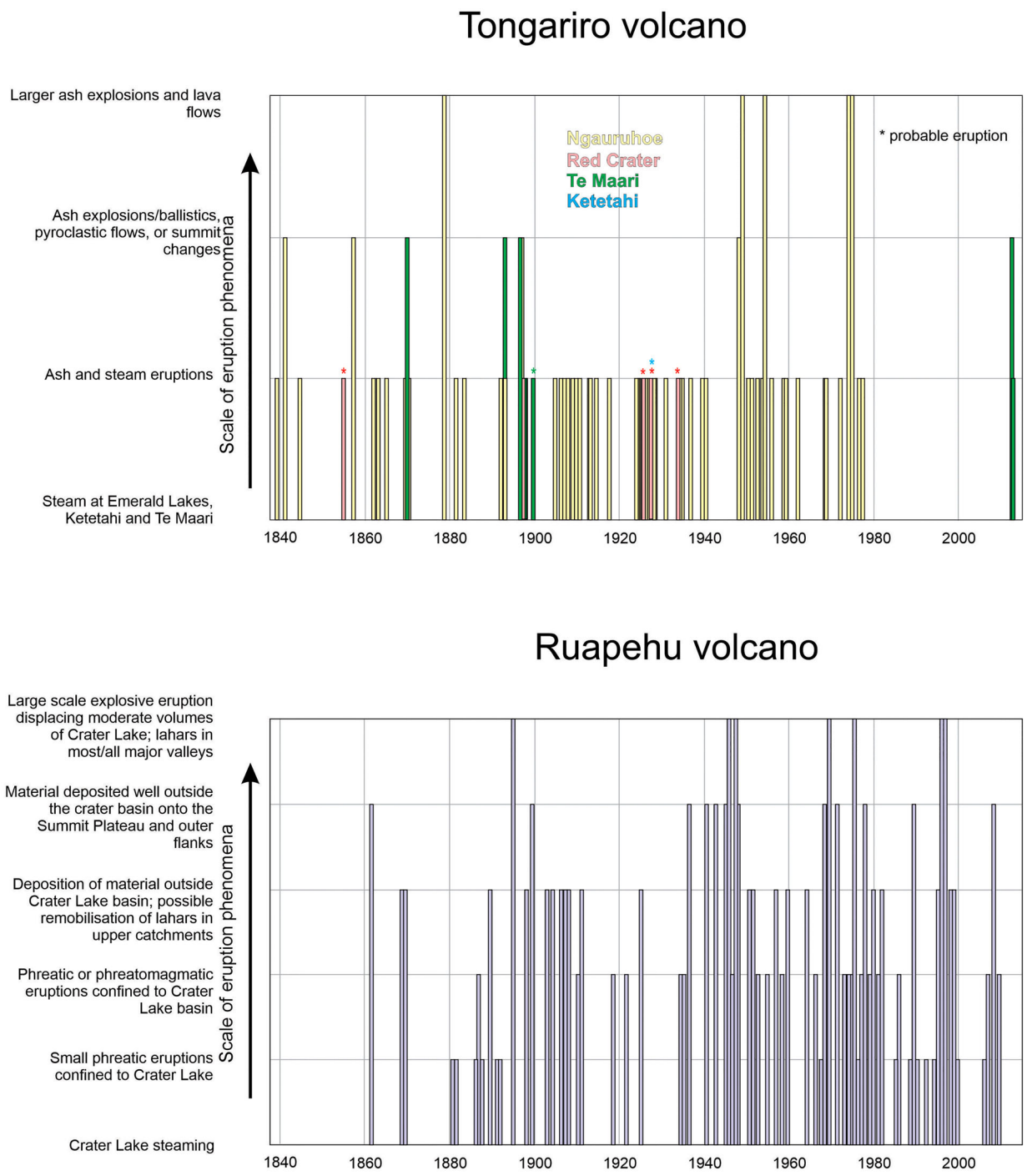

Figure 15. Timing and scales of historic eruptions at Tongariro and Ruapehu volcanoes. Eruptions at Tongariro are coloured by the active vent. The largest examples of historic events at both volcanoes reach the equivalent of Volcanic Explosivity Index 3 (VEI: Newhall and Self 1982). Modified from Townsend et al. (2017).

et al. 2014; Lube et al. 2014; Procter et al. 2014; Turner et al. 2014). An example of hazard interaction was seen in the 2012 Te Maari eruptions where a debris avalanche blocked a small stream and formed a dam that failed two months later, producing a lahar that reached Highway 46 (Walsh et al. 2016). The timing, footprint and intensity of the hazards associated with small steam-driven eruptions are now much better understood, but can still be difficult to forecast and apply at specific vents to determine, for example, the ballistic block hazard at Red Crater (Gates 2018). Ballistic blocks from the August 2012 Te Maari explosion reached a maximum distance of 2.3 km, beyond the then-current 2 km radius hazard zones used in the National Park hazard maps (Fitzgerald et al. 2014).

On Ruapehu, eruptions through Te Wai ā-Moe/Crater Lake may lead directly to lahars down the Whangaehu River (Manville and Cronin 2007). Material erupted onto the summit plateau (combined with snow when present) can form lahars into the Whakapapa and upper Turoa Ski areas (Carrivick

et al. 2009). Detection of an eruption leads to automated lahar warnings for the Whangaehu River catchment (Keys 2007) and the Whakapapa ski area, both of which may be affected within minutes of an explosive eruption (Sherburn and Bryan 1999). Paton et al. (1998) critiqued the organisational response to the 1995–96 Ruapehu eruptions and more recent integration of risk management with eruption response planning at Ruapehu was explored by Keys and Green (2010). Hazard management for these relatively small scale steam-driven eruptions in areas frequented by tourists remains a challenge worldwide.

Larger magmatic eruptions

Larger magmatic eruptions in many cases generate more precursory signals (Bryan and Sherburn 1999), yet the longer duration and episodic nature of such eruptions pose additional challenges (cf. Aspinall et al. 2002). The durations and magnitudes of specific hazards are harder to forecast, particularly with observations limited by the few historic examples (Houghton et al. 1987). Isopachs and isopleths from deposits produced by a range of magmatic eruption styles at Tongariro and Ruapehu provide an approximate guide to potential tephra hazard scenarios (Topping 1973; Donoghue et al. 1995a; Donoghue and Neall 1996; Bonadonna et al. 2005; Pardo et al. 2012a, 2012b, 2014; Heinrich et al. 2020a). At Ruapehu, hazard modelling has improved scenario development for larger eruptions, with a focus on ash fall and lahars (Cronin et al. 1998; Hurst and Turner 1999; Turner and Hurst 2001; Lecointre et al. 2004; Manville and Cronin 2007; Carrivick et al. 2009; Graettinger et al. 2010; Procter et al. 2010, 2012; Liu et al. 2015).

Additional worst-case scenarios relating to debris avalanches and edifice collapse have also been investigated (Schaefer et al. 2018). Large eruptions from Ruapehu have been inferred from preserved pyroclastic density current deposits (Donoghue et al. 1995b; Pardo et al. 2014; Cowlyn 2016; Gillies 2018) although constraining the hazard footprints associated with such eruptions is challenging because deposits are poorly preserved (Cowlyn 2016; Gillies 2018). It has been suggested that pyroclastic density currents could be a hazard from even small explosive events (Degruyter and Bonadonna 2013). Minor pyroclastic density currents driven by eruption-column collapse occurred in the 1945 eruption (Figure 16), and current skifield infrastructure is well within the hazard zones of pyroclastic density currents and lava flows (Cowlyn 2016).

Impact and mitigation

Volcanic impact studies from Tongariro and the 1995–1996 Ruapehu eruptions have focused on health, agriculture and critical infrastructure, (Cronin et al. 1997c, 1998, 2003; Johnston et al. 2000; Stewart et al. 2006; Hitchcock and Cole 2007; Wilson and Cole 2007; Becker et al. 2010; Newnham et al. 2010). Mitigation measures are generally avoidance, land-use planning, structural protection and warning. Land use planning has largely been accomplished as a by-product of the existence of the National Park (Becker et al. 2010; Keys and Green 2010).

At Ruapehu, some structural mitigation has been undertaken in the Whangaehu River channel. After the 1945 eruption, Te Wai ā-Moe/Crater Lake refilled until an ice barrier broke on 24 December 1953 (Manville 2004). The resulting lahar caused the Tangiwai disaster, in which 151 people were killed, by destroying a railway bridge as an express train approached it. As the lake again refilled following the 1995–96 eruptions, the hazard of another lahar was alleviated by a warning system, which detected the breakout that occurred on 18 March 2007, and stopped road and rail traffic. Prior to the 2007 lahar, the road bridge at Tangiwai was also altered and raised to provide better clearance, and a levee was built to prevent any lahar from overspilling into the northern catchment draining to Lake Taupo.

Because of the strong public interest in tourism in TNP not all risk can be avoided, risk being a function of hazard and the likelihood and severity of its impacts. With the exposure of people to volcanic hazards there will always be some probability of adverse impacts including severe injury and death. Mitigation of that probability and impact has mostly involved education and provision of warnings (where possible; see 'steam-driven eruptions' above). Geophysical monitoring through the GeoNet project (http://geonet.org.nz) has become iteratively more intensive and diverse over recent decades. Monitoring information and eruption forecasts through Volcanic Alert Bulletins are provided by the volcano monitoring group at GNS Science. Volcanic Alert Levels are also used and they have been updated in the last 6 years based on social science evidence, to include two unrest levels and hazard descriptors (Potter et al. 2014). Risk-management is led by the Department of Conservation and local Civil Defence and Emergency Managers. They provide planning, active risk management, and risk awareness and self-protection advice through signage, public education, hazard maps and drills (Leonard et al. 2014). Recent work has analysed the advantages of also including mātauranga Māori (tribal knowledge) in emergency management in the park (Gabrielsen et al. 2017).

In developing warnings, volcanologists have partnered with social scientists, learning from 15 years of survey and observation data on warnings to characterise and quantify human awareness and responses at Ruapehu and Tongariro volcanoes (e.g. Leonard

Figure 16. Photographs to illustrate the range and scale of hazards resulting from recent eruptions at Ruapehu and Tongariro. **A**: PDC (white arrow) formed from eruption-column collapse during the 1945 Ruapehu eruption, looking northeast from Raetihi (Photo: N. Mosen, Lansdown Collection). **B**: Aftermath of the Tangiwai Disaster on 24 December 1953, following the 1945 eruption of Ruapehu volcano. The Whangaehu River was occupied by a lahar from the collapse of the Te Wai-ā-Moe/Crater Lake outlet barrier, washing away the bridge with the train and carrying carriages downstream. Source: Peacock, Morice Gladstone, 1916–1995: Negatives, prints, register and minute book from twentieth Century Photography studio, Taumarunui. Ref: MP-0059-11-F. Alexander Turnbull Library, Wellington, New Zealand. /records/22808804. **C**: Ice slurry lahar deposit from the September 23, 1995 Ruapehu eruption alongside the Far West T-Bar on Whakapapa Ski Area (Photo: GNS Science). **D**: An ice slurry lahar deposit from the 25 September 2007 Ruapehu eruption narrowly missed this snow groomer on Whakapapa Ski Area, adjacent to the Far West T-Bar (Photo: Graham Leonard, GNS Science). **E**: Crater formed by a ballistic block launched 1.4 km during the August 6, 2012 Tongariro eruption at Te Maari (Photo: Rebecca Fitzgerald); **F**: Damage to the ceiling and bunks of the Ketetahi Hut from Te Maari ballistic block impacts 1.4 km from the vent during the August 6 2012 eruption (Photo: Nick Kennedy).

et al. 2008, 2014). Evacuation drills for Whakapapa Ski Area are conducted annually, and a persistent minority of people do not move to safety, or do not move quickly enough, from year to year. Whilst the majority of risk factors in the case of lahars in Whakapapa ski area can be mitigated through warnings, a residual risk is hard to eliminate (Leonard et al. 2008).

Conclusions

Over the last 50 years a large volume of diverse Earth science research has been conducted in and around Tongariro National Park focussed on the volcanoes, the volcanic and regional structure, and the basement geology. Many dozens of graduate student theses and hundreds of academic papers have been published.

Andesite has been erupting in this area for at least 1 million years. Petrological and geophysical studies have clearly delineated and characterised the basement greywacke, and have identified potential zones of magma storage, fluid ascent and hydrothermal alteration in the greywacke, overlying Tertiary mudstones and the TNP volcanics. The geochemical origins of magmas and their relationship to the basement are well characterised, and the evolution and cyclicity of magmatism have been placed into a comprehensive geochronology. The magma systems for Ruapehu and Tongariro are independent, at least in the upper crust. The hydrothermal system at Ruapehu is now focussed on Te Wai ā-Moe/Crater Lake, but is more distributed at Tongariro where the individual systems are not connected at depth. There is an association of faulting with volcanism, with correlations and influences between the two over time. Glaciers have resided on the volcanoes for the majority of their histories. Volcano-glacier interactions have been shown to directly control the morphologies of the volcanic edifices and strongly influence the rates of edifice growth and sedimentation on the surrounding ring plains. Historic unrest and eruptions are well documented and linked to ever-improving geophysical and geochemical documentation and modelling. Both volcanoes pose a hazard from rapid-onset, unheralded small eruptions.

The proximity of Ruapehu to Tongariro is deceptive, as they have distinct structures and magma systems, which partly relate to their structural settings. The Ruapehu edifice, with less influence from rifting processes, is large and tall enough to create its own tectonic regime: it is associated with wide-set enveloping faults mostly well outside the limits of the edifice, and magma is focussed into a central area. As a result, Ruapehu has erupted more dacite magmas than Tongariro due to extensive crustal assimilation and fractional crystallisation through a central magma plumbing axis. Ruapehu typically shows evidence for magma mixing resulting from the interaction between recharging and stalled magmas (sometimes directly leading to eruption: Conway et al. 2020). At Tongariro, the extension rate is greater, the volcano is traversed by several faults parallel to the Taupo Rift orientation and cone building has occurred over a wider area, leading to a less unified edifice without a central focus.

There are several areas of desirable future work to highlight here:

1) Full integration of the evolution of the ring plain and pyroclastic histories with the on-mountain lava and moraine records.
2) Re-evaluation of the structural controls on faulting at the Taupo Rift termination in light of updated fault mapping.
3) Acquisition of higher resolution imaging of mid- and deep-crustal structure and magma sources associated with Ruapehu and Tongariro using MT and seismic methods.
4) Development of a unified structural-magma-hydrothermal-eruption system model. This could be achieved by integrating geophysical techniques (seismic monitoring, geomagnetic imaging and deformation via GNSS coupled to InSAR), geochemistry (gas and fluid monitoring in real-time) with contemporary developments in petrology, including microsampling (micro drilling) and micro-scale analysis of minerals and glasses for diffusion modelling. In particular, application of mineral geothermobarometers and diffusion chronometers will help constrain interpretations of where magma is assembled and stored in the crust, and how quickly it ascends to the vents. These parameters are critical in the context of hazard assessment during future unrest or eruptions.
5) Revision of eruption probabilities and interpretations of eruption mechanisms using the extensive monitoring datasets collected over recent decades.
6) Development of robust models for eruptive processes of the volcanoes, representing all historic volcanic phenomena, which quantify the multiple hazards and bring them together to provide unified hazard and impact metrics. These hazard metrics can then be combined with both short and long-term monitoring and geological data in a probabilistic model to produce forecasts for different phenomena or scenarios.
7) Provision of monitoring and hazard data to allow flexible management of risk in a modern environment of economic and political pressure. The risks from sudden-onset steam-driven eruptions remain an acute challenge, more particularly at Ruapehu, as does managing uncertainty around unrest, duration and the episodicity of larger magmatic eruptions.

Acknowledgements

We would like to particularly acknowledge Prof. Jim Cole (ex. University of Canterbury), Dr Harry Keys (ex. Department of Conservation – DOC) and Prof. Richard Price (ex University of Waikato) for their long-term roles in understanding NZ andesites and in supporting Earth science research in the park over many decades. We highlight the many dozens of graduate students who have contributed to the understanding of Ruapehu and Tongariro, especially the seminal works of Bill Hackett and Barbara Hobden, respectively, on these two volcanoes. More recently we note the work of Adam Belkadi, James Cowlyn, Becs Fitzgerald, Stephanie Gates, Janina Gillies, Martha Gabriela (Gaby) Gómez-Vasconcelos, Mirja Heinrich, Stan Mordensky, Lauren Schaefer, Manuela Tost and Marija Voloschina. Research at TNP has been enthusiastically supported, with abundant field assistance, by many DOC staff, especially Hollei Gabrielsen (Ngāti Rangi), Nicki (Shorty) Hughes and Blake McDavitt, as well as by Bubs Smith (Ngāti Hikairo). We thank Victoria University, Department of Conservation and EQC for funding support for the PhD studies of Conway and Pure, and other New Zealand universities for similar support of past students over the years. We finally acknowledge the thoughtful reviews by Tod Waight and one anonymous reviewer that improved this manuscript.

Data availability statement

Data sharing is not applicable to this article as no new data were created or analysed in this study.

Disclosure statement

No potential conflict of interest was reported by the author(s).

Funding

We thank the GNS Science MBIE-funded Strategic Science Investment Fund (SSIF) and its predecessors, and the Resilience to Nature's Challenges National Science Challenge and its predecessor the MBIE-funded Natural Hazard Research Platform for financial support.

ORCID

Graham S. Leonard http://orcid.org/0000-0002-4859-0180
Rosie P. Cole http://orcid.org/0000-0003-2405-0240
Shane J. Cronin http://orcid.org/0000-0001-7499-603X
Craig A. Miller http://orcid.org/0000-0001-8499-0352
James D. L. White http://orcid.org/0000-0002-2970-711X
Colin J. N. Wilson http://orcid.org/0000-0001-7565-0743

References

Adams CJ, Mortimer N, Campbell HJ, Griffin WL. 2009. Age and isotopic characterisation of metasedimentary rocks from the Torlesse Supergroup and Waipapa Group in the central North Island, New Zealand. New Zealand Journal of Geology and Geophysics. 52:149–170.

Aspinall WP, Loughlin SC, Michael FV, Miller AD, Norton GE, Rowley KC, Sparks RSJ, Young SR. 2002. The Montserrat Volcano Observatory: its evolution, organization, role and activities. Geological Society of London Memoirs. 21:71–91.

Auer A, Martin CE, Palin JM, White JDL, Nakagawa M, Stirling C. 2015. The evolution of hydrous magmas in the Tongariro Volcanic Centre: the 10 ka Pahoka-Mangamate eruptions. New Zealand Journal of Geology and Geophysics. 58:364–384.

Auer A, White JDL, Manville V. 2012. Cryptic eruption of Mount Ruapehu revealed by deposits of sediment laden streamflow in a steep mountain valley: The 4 ka Kiwikiwi Formation, Whangaehu Valley, NZ. Journal of Volcanology and Geothermal Research. 243:45–58.

Auer A, White JDL, Nakagawa M, Rosenberg MD. 2013. Petrological record from young Ruapehu eruptions in the 4.5 ka Kiwikiwi Formation, Whangaehu Gorge, New Zealand. New Zealand Journal of Geology and Geophysics. 56:121–133.

Auer A, White JDL, Tobin MJ. 2016. Variable H_2O content in magmas from the Tongariro Volcanic Centre and its relation to crustal storage and magma ascent. Journal of Volcanology and Geothermal Research. 325:203–210.

Barker SJ, Rowe MC, Wilson CJN, Gamble JA, Rooyakkers SM, Wysoczanski RJ, Illsley-Kemp F, Kenworthy CC. 2020. What lies beneath? Reconstructing the primitive magmas fueling voluminous silicic volcanism using olivine-hosted melt inclusions. Geology. 48:504–508.

Battey MH. 1949. The recent eruption of Ngauruhoe. Records of the Auckland Institute and Museum. 3:387–395.

Becker JS, Saunders WSA, Robertson CM, Leonard GS, Johnston DM. 2010. A synthesis of challenges and opportunities for reducing volcanic risk through land use planning in New Zealand. Australasian Journal of Disaster and Trauma Studies. 2010-1. http://trauma.massey.ac.nz/issues/2010-1/becker.htm.

Beetham RD, Watters WA. 1985. Geology of Torlesse and Waipapa terrane basement rocks encountered during the Tongariro power development project, North Island, New Zealand. New Zealand Journal of Geology and Geophysics. 28:575–594.

Beier C, Haase KM, Brandl PA, Krumm SH. 2017. Primitive andesites from the Taupo Volcanic Zone formed by magma mixing. Contributions to Mineralogy and Petrology. 172:33.

Bonadonna C, Phillips JC, Houghton BF. 2005. Modeling tephra sedimentation from a Ruapehu weak plume eruption. Journal of Geophysical Research. 110:B08209.

Breard ECP, Lube G, Cronin SJ, Fitzgerald R, Kennedy B, Scheu B, Montanaro C, White JDL, Tost M, Procter JN, Moebis A. 2014. Using the spatial distribution and lithology of ballistic blocks to interpret eruption sequence and dynamics: August 6 2012 Upper Te Maari eruption, New Zealand. Journal of Volcanology and Geothermal Research. 286:373–386.

Browne GH. 2004. Late Neogene sedimentation adjacent to the tectonically evolving North Island axial ranges: insights from Kuripapango, western Hawke's Bay. New Zealand Journal of Geology and Geophysics. 47:663–674.

Bryan CJ, Sherburn S. 1999. Seismicity associated with the 1995–1996 Eruptions of Ruapehu volcano, New Zealand: narrative and insights into physical processes. Journal of Volcanology and Geothermal Research. 90:1–18.

Cameron E, Gamble J, Price R, Smith I, McIntosh W, Gardner M. 2010. The petrology, geochronology and geochemistry of Hauhungatahi volcano, S.W. Taupo Volcanic Zone. Journal of Volcanology and Geothermal Research. 190:179–191.

Carrivick JL, Manville V, Cronin SJ. 2009. A fluid dynamics approach to modelling the 18th March 2007 lahar at Mt. Ruapehu, New Zealand. Bulletin of Volcanology. 71:153–169.

Cashman KV. 1979. Evolution of Kakaramea and Maungakatote volcanoes, Tongariro Volcanic Centre, New Zealand. [MSc thesis]. Wellington, New Zealand: Victoria University of Wellington.

Cassidy J, Ingham M, Locke CA, Bibby H. 2009. Subsurface structure across the axis of the Tongariro Volcanic Centre, New Zealand. Journal of Volcanology and Geothermal Research. 179:233–240.

Christenson BW. 2000. Geochemistry of fluids associated with the 1995–1996 Eruption of Mt. Ruapehu, New Zealand: signatures and processes in the magmatic-hydrothermal system. Journal of Volcanology and Geothermal Research. 97:1–30.

Christenson BW, Reyes AG, Young R, Moebis A, Sherburn S, Cole-Baker J, Britten K. 2010. Cyclic processes and factors leading to phreatic eruption events: insights from the 25 September 2007 eruption through Ruapehu Crater Lake, New Zealand. Journal of Volcanology and Geothermal Research. 191:15–32.

Christenson BW, Wood CP. 1993. Evolution of a vent-hosted hydrothermal system beneath Ruapehu Crater Lake, New Zealand. Bulletin of Volcanology. 55:547–565.

Clark RH. 1960. Appendix II: Petrology of the volcanic rocks of Tongariro Subdivision. In: Gregg DR. Geology of the Tongariro Subdivision. New Zealand Geological Survey Bulletin. 40:107–123.

Cole JW. 1978. Andesites of the Tongariro Volcanic Centre, North Island, New Zealand. Journal of Volcanology and Geothermal Research. 3:121–153.

Cole JW, Cashman KV, Rankin PC. 1983. Rare-earth element geochemistry and the origin of andesites and basalts of the Taupo Volcanic Zone, New Zealand. Chemical Geology. 38:255–274.

Cole SE, Cronin SJ, Sherburn S, Manville V. 2009. Seismic signals of snow-slurry lahars in motion: 25 September 2007, Mt Ruapehu, New Zealand. Geophysical Research Letters. 36:L09405.

Cole JW, Lewis KB. 1981. Evolution of the Taupo-Hikurangi subduction system. Tectonophysics. 72:1–21.

Cole JW, Nairn IA. 1975. Catalogue of the active volcanoes of the world including solfatara fields. Part 22: New Zealand. International Association of Volcanology and Chemistry of the Earth's Interior, Rome

Cole RP, Ohneiser C, White JDL, Townsend DB, Leonard GS. 2019. Paleomagnetic evidence for cold emplacement of eruption-fed density current deposits beneath an ancient summit glacier, Tongariro volcano, New Zealand. Earth and Planetary Science Letters. 522:155–165.

Cole RP, White JDL, Conway CE, Leonard GS, Townsend DB, Pure LR. 2018. The glaciovolcanic evolution of an andesitic edifice, South Crater, Tongariro volcano, New Zealand. Journal of Volcanology and Geothermal Research. 352:55–77.

Cole RP, White JDL, Townsend DB, Leonard GS, Conway CE. 2020. Glaciovolcanic emplacement of an intermediate hydroclastic breccia-lobe complex during the penultimate glacial period (190−130 ka), Ruapehu volcano, New Zealand. Geological Society of America Bulletin. 132:1903–1913.

Conway CE. 2016. Studies on the glaciovolcanic and magmatic evolution of Ruapehu volcano, New Zealand [PhD thesis]. Wellington, New Zealand: Victoria University of Wellington, 259 p.

Conway CE, Chamberlain KJ, Harigane Y, Morgan, DJ, Wilson CJN. 2020. Rapid assembly of high-Mg andesites and dacites by magma mixing at a continental arc stratovolcano. Geology. 48:1033–1037.

Conway CE, Gamble JA, Wilson CJN, Leonard GS, Townsend DB, Calvert AT. 2018. New petrological, geochemical and geochronological perspectives on andesite-dacite magma genesis at Ruapehu volcano, New Zealand. American Mineralogist. 103:565–581.

Conway CE, Leonard GS, Townsend DB, Calvert AT, Wilson CJN, Gamble JA, Eaves SR. 2016. A high resolution $^{40}Ar/^{39}Ar$ lava chronology and construction history for Ruapehu volcano, New Zealand. Journal of Volcanology and Geothermal Research. 327:152–179.

Conway CE, Townsend DB, Leonard GS, Wilson CJN, Calvert AT, Gamble JA. 2015. Lava-ice interaction on a large composite volcano: a case study from Ruapehu, New Zealand. Bulletin of Volcanology. 77:21.

Cowlyn JD. 2016. Pyroclastic density currents at Ruapehu volcano. [PhD thesis]. Christchurch, New Zealand: University of Canterbury. 268 p.

Cronin SJ, Hedley MJ, Neall VE, Smith RG. 1998. Agronomic impact of tephra fallout from the 1995 and 1996 Ruapehu Volcano eruptions, New Zealand. Environmental Geology. 34:21–30.

Cronin SJ, Hedley MJ, Smith RG, Neall VE. 1997c. Impact of Ruapehu ash fall on soil and pasture nutrient status 1. October 1995 eruptions. New Zealand Journal of Agricultural Research. 40:383–395.

Cronin SJ, Neall VE. 1997. A late Quaternary stratigraphic framework for the northeastern Ruapehu and eastern Tongariro ring plains. New Zealand. New Zealand Journal of Geology and Geophysics. 40:185–197.

Cronin SJ, Neall VE, Lecointre JA, Hedley MJ, Loganathan P. 2003. Environmental hazards of fluoride in volcanic ash: a case study from Ruapehu volcano, New Zealand. Journal of Volcanology and Geothermal Research. 121:271–291.

Cronin SJ, Neall VE, Lecointre JA, Palmer AS. 1996b. Unusual "snow slurry" lahars from Ruapehu volcano, New Zealand, September 1995. Geology. 24:1107–1110.

Cronin SJ, Neall VE, Lecointre JA, Palmer AS. 1997b. Changes in Whangaehu River lahar characteristics during the 1995 eruption sequence, Ruapehu volcano, New Zealand. Journal of Volcanology and Geothermal Research. 76:47–61.

Cronin SJ, Neall VE, Palmer AS. 1996a. Geological history of the north-eastern ring plain of Ruapehu volcano, New Zealand. Quaternary International. 34–36:21–28.

Cronin SJ, Neall VE, Palmer AS, Stewart RB. 1997a. Methods of identifying late Quaternary rhyolitic tephras on the ring plains of Ruapehu and Tongariro volcanoes, New Zealand. New Zealand Journal of Geology and Geophysics. 40:175–184.

Crouch JF, Pardo N, Miller CA. 2014. Dual polarisation C-band weather radar imagery of the 6 August 2012 Te Maari eruption, Mount Tongariro, New Zealand. Journal of Volcanology and Geothermal Research. 286:415–436.

Degruyter W, Bonadonna C. 2013. Impact of wind on the condition for column collapse of volcanic plumes. Earth and Planetary Science Letters. 377:218–226.

Dibble RR. 1974. Volcanic seismology and accompanying activity of Ruapehu volcano, New Zealand. In: Civetta L, Gasparini P, Luongo G, Rapolla A, editors. Physical volcanology. Amsterdam: Elsevier; p. 49–85.

Donoghue SL, Gamble JA, Palmer AS, Stewart RB. 1995b. Magma mingling in an andesite pyroclastic flow of the Pourahu Member, Ruapehu volcano, New Zealand. Journal of Volcanology and Geothermal Research. 68:177–191.

Donoghue SL, Neall VE. 1996. Tephrostratigraphic studies at Tongariro volcanic centre, New Zealand: an overview. Quaternary International. 34–36:13–20.

Donoghue SL, Neall VE. 2001. Late Quaternary constructional history of the southeastern Ruapehu ring plain, New Zealand. New Zealand Journal of Geology and Geophysics. 44:439–466.

Donoghue SL, Neall VE, Palmer AS. 1995a. Stratigraphy and chronology of late Quaternary andesitic tephra deposits, Tongariro Volcanic Centre, New Zealand. Journal of the Royal Society of New Zealand. 25:115–206.

Donoghue SL, Neall VE, Palmer AS, Stewart RB. 1997. The volcanic history of Ruapehu during the past 2 millennia based on the record of Tufa Trig tephras. Bulletin of Volcanology. 59:136–146.

Donoghue SL, Vallance J, Smith IE, Stewart RB. 2007. Using geochemistry as a tool for correlating proximal andesitic tephra: case studies from Mt Rainier (USA) and Mt Ruapehu (New Zealand). Journal of Quaternary Science. 22:395–410.

Eaves S, Mackintosh AN, Anderson BM, Doughty AM, Townsend DB, Conway CE, Winckler G, Schaefer JM, Leonard GS, Calvert AT. 2016b. The Last Glacial Maximum in central North Island, New Zealand: palaeoclimate inferences from glacier modelling. Climate of the Past. 12:943–943.

Eaves SR, Mackintosh AN, Winckler G, Schaefer JM, Alloway BV, Townsend DB. 2016a. A cosmogenic 3He chronology of late Quaternary glacier fluctuations in North Island, New Zealand (39° S). Quaternary Science Reviews. 132:40–56.

Eaves SR, Winckler G, Schaefer JM, Vandergoes MJ, Alloway BV, Mackintosh AN, Townsend DB, Ryan MT, Li X. 2015. A test of the cosmogenic ^{3}He production rate in the south-west Pacific (39° S). Journal of Quaternary Science. 30:79–87.

Eberhart-Phillips D, Bannister S, Reyners M. 2020. Attenuation in the mantle wedge beneath super-volcanoes of the Taupo Volcanic Zone, New Zealand. Geophysical Journal International. 220:703–723.

Fitzgerald RH, Tsunematsu K, Kennedy BM, Breard ECP, Lube G, Wilson TM, Jolly AD, Pawson J, Rosenberg MD, Cronin SJ. 2014. The application of a calibrated 3D ballistic trajectory model to ballistic hazard assessments at Upper Te Maari, Tongariro. Journal of Volcanology and Geothermal Research. 286:248–262.

Gabrielsen H, Procter J, Rainforth H, Black T, Harmsworth G, Pardo N. 2017. Reflections from an indigenous community on volcanic event management, communications and resilience. In: Fearnley CJ, Bird DK, Haynes K, McGuire WJ, Jolly G, editor. Observing the volcano world. Advances in Volcanology (An official book series of the International Association of Volcanology and Chemistry of the Earth's Interior – IAVCEI, Barcelona, Spain). Cham: Springer; p. 463–479.

Gamble JA, Price RC, Smith IEM, McIntosh WC, Dunbar NW. 2003. ^{40}Ar/^{39}Ar geochronology of magmatic activity, magma flux and hazards at Ruapehu Volcano, Taupo Volcanic Zone, New Zealand. Journal of Volcanology and Geothermal Research. 120:171–187.

Gamble JA, Wood CP, Price RC, Smith IEM, Stewart RB, Waight T. 1999. A fifty year perspective of magmatic evolution on Ruapehu Volcano, New Zealand: verification of open system behaviour in an arc volcano. Earth and Planetary Science Letters. 170:301–314.

Gates SL. 2018. Mapping and modelling phreatic ballistic fields at tourism hotspots: a methodological assessment at Tongariro and Whakaari (White Island) volcanoes, New Zealand. [MSc thesis.] Christchurch, New Zealand: University of Canterbury. 143 p.

Giggenbach W. 1974. The chemistry of Crater Lake, Mt. Ruapehu (New Zealand) during and after the 1971 active period. New Zealand Journal of Science. 17:33–45.

Giggenbach WF, Glover RB. 1975. The use of chemical indicators in the surveillance of volcanic activity affecting the crater lake on Mt Ruapehu. New Zealand. Bulletin Volcanologique. 39:70–81.

Gill J. 1981. Orogenic andesites and plate tectonics. Springer, Berlin. 390 p.

Gillies J. 2018. Identifying pyroclastic density currents from partial outcrop exposure at Mt Ruapehu, New Zealand. [MSc thesis.] Christchurch, New Zealand, University of Canterbury. 71 p.

Godfrey HJ, Fry B, Savage MK. 2017. Shear-wave velocity structure of the Tongariro Volcanic Centre, New Zealand: fast Rayleigh and slow Love waves indicate strong shallow anisotropy. Journal of Volcanology and Geothermal Research. 336:33–50.

Gómez-Vasconcelos MG, Villamor P, Cronin S, Palmer A, Procter J, Stewart RB. 2020. Spatio-temporal associations between dike intrusions and fault ruptures in the Tongariro Volcanic Center, New Zealand. Journal of Volcanology and Geothermal Research. 404:107037.

Gómez-Vasconcelos MG, Villamor P, Cronin S, Procter J, Palmer A, Townsend D, Leonard G. 2017. Crustal extension in the Tongariro graben, New Zealand: insights into volcano-tectonic interactions and active deformation in a young continental rift. Geological Society of America Bulletin. 129:1085–1099.

Graettinger AH, Manville V, Briggs RM. 2010. Depositional record of historic lahars in the upper Whangaehu Valley, Mt. Ruapehu, New Zealand: implications for trigger mechanisms, flow dynamics and lahar hazards. Bulletin of Volcanology. 72:279–296.

Graham IJ. 1987. Petrography and origin of metasedimentary xenoliths in lavas from Tongariro Volcanic Centre, New Zealand. New Zealand Journal of Geology and Geophysics. 30:139–157.

Graham IJ, Blattner P, McCulloch MT. 1990. Meta-igneous granulite xenoliths from Mount Ruapehu, New Zealand: fragments of altered oceanic crust? Contributions to Mineralogy and Petrology. 105:650–661.

Graham IJ, Grapes RH, Kifle K. 1988. Buchitic metagraywacke xenoliths from Mount Ngauruhoe, Taupo Volcanic Zone, New Zealand. Journal of Volcanology and Geothermal Research. 35:205–216.

Graham IJ, Hackett WR. 1987. Petrology of calc-alkaline lavas from Ruapehu volcano and related vents, Taupo Volcanic zone. Journal of Petrology. 28:531–567.

Gregg DR. 1960. Geology of Tongariro subdivision. New Zealand Geological Survey Bulletin. ns 40.

Greve A, Turner GM, Conway CE, Townsend DB, Gamble JA, Leonard GS. 2016. Palaeomagnetic refinement of the eruption ages of Holocene lava flows, and implications for the eruptive history of the Tongariro Volcanic Centre, New Zealand. Geophysical Supplements to the Monthly Notices of the Royal Astronomical Society. 207:702–718.

Hackett WR, Houghton BF. 1989. A facies model for a Quaternary andesite volcano, Ruapehu, New Zealand. Bulletin of Volcanology. 51:51–68.
Hagerty M, Benites R. 2003. Tornillos beneath Tongariro Volcano, New Zealand. Journal of Volcanology and Geothermal Research. 125:151–169.
Hamling IJ. 2021. InSAR observations over the Taupō Volcanic Zone's cone volcanoes: insights and challenges from the New Zealand volcano supersite. New Zealand Journal of Geology and Geophysics. 64(2–3):347–357. doi: 10.1080/00288306.2020.1721545.
Hamling IJ, Williams CA, Hreinsdóttir S. 2016. Depressurization of a hydrothermal system following the August and November 2012 Te Maari eruptions of Tongariro, New Zealand. Geophysical Research Letters. 43:168–175.
Harrison A, White RS. 2006. Lithospheric structure of an active backarc basin: the Taupo Volcanic Zone, New Zealand. Geophysical Journal International. 167:968–990.
Hayes G, Reyners M, Stuart G. 2004. The Waiouru, New Zealand, earthquake swarm: persistent mid crustal activity near an active volcano. Geophysical Research Letters. 31:L19613.
Heinrich M, Cronin SJ, Pardo N. 2020a. Understanding multi-vent Plinian eruptions at Mt. Tongariro volcanic complex, New Zealand. Bulletin of Volcanology. 82:30.
Heinrich M, Cronin SJ, Torres-Orozco R, Colombier M, Scheu B, Pardo N. 2020b. Micro-porous pyroclasts reflecting multi-vent basaltic-andesite plinian eruptions at Mt. Tongariro, New Zealand. Journal of Volcanology and Geothermal Research. 401:106936.
Hill GJ, Bibby HM, Ogawa Y, Wallin EL, Bennie SL, Caldwell TG, Keys H, Bertrand EA, Heise W. 2015. Structure of the Tongariro volcanic system: insights from magnetotelluric imaging. Earth and Planetary Science Letters. 432:115–125.
Hitchcock DW, Cole JW. 2007. Potential impacts of a widespread subplinian andesitic eruption from Tongariro volcano, based on a study of the Poutu Lapilli. New Zealand Journal of Geology and Geophysics. 50:53–66.
Hobden BJ. 1997. Modelling magmatic trends in space and time: eruptive and magmatic history of the Tongariro Volcanic Complex PhD [Thesis]. Christchurch, New Zealand: University of Canterbury, 508 p.
Hobden BJ, Houghton BF, Davidson JP, Weaver SD. 1999. Small and short-lived magma batches at composite volcanoes: time windows at Tongariro volcano, New Zealand. Journal of the Geological Society, London. 156:865–868.
Hobden BJ, Houghton BF, Lanphere MA, Nairn IA. 1996. Growth of the Tongariro Volcanic Complex: new evidence from K-Ar age determinations. New Zealand Journal of Geology and Geophysics. 39:151–154.
Hobden BJ, Houghton BF, Nairn IA. 2002. Growth of a young, frequently active composite cone: Ngauruhoe Volcano, New Zealand. Bulletin of Volcanology. 64:392–409.
Houghton BF, Hackett WR. 1984. Strombolian and phreatomagmatic deposits of Ohakune Craters, Ruapehu, New Zealand: a complex interaction between external water and rising basaltic magma. Journal of Volcanology and Geothermal Research. 21:207–231.
Houghton BF, Latter JH, Hackett WR. 1987. Volcanic hazard assessment for Ruapehu composite volcano, Taupo Volcanic Zone, New Zealand. Bulletin of Volcanology. 49:737–751.
Hurst AW, Bibby HM, Scott BJ, McGuinness MJ. 1991. The heat source of Ruapehu Crater Lake; deductions from the energy and mass balances. Journal of Volcanology and Geothermal Research. 46:1–20.
Hurst T, Heise W, Hreinsdottir S, Hamling I. 2016. Geophysics of the Taupo Volcanic Zone: a review of recent developments. Geothermics. 59:188–204.
Hurst T, Jolly AD, Sherburn S. 2014. Precursory characteristics of the seismicity before the 6 August 2012 eruption of Tongariro volcano, North Island, New Zealand. Journal of Volcanology and Geothermal Research. 286:294–302.
Hurst T, Kilgour G, Hamling I. 2018. Magmatic triggering of earthquakes on distal faults as a potential medium-term warning signal from Ruapehu volcano. Geophysical Research Letters. 45:12776–12783.
Hurst AW, McGinty PJ. 1999. Earthquake swarms to the west of Mt Ruapehu preceding its 1995 eruption. Journal of Volcanology and Geothermal Research. 90:19–28.
Hurst AW, Sherburn S. 1993. Volcanic tremor at Ruapehu: characteristics and implications for the resonant source. New Zealand Journal of Geology and Geophysics. 36:475–485.
Hurst AW, Turner R. 1999. Performance of the program ASHFALL for forecasting ashfall during the 1995 and 1996 eruptions of Ruapehu volcano. New Zealand Journal of Geology and Geophysics. 42:615–622.
Illsley-Kemp F, Savage MK, Wilson CJN, Bannister S. 2019. Mapping stress and structure from subducting slab to magmatic rift: crustal seismic anisotropy of the North Island, New Zealand. Geochemistry, Geophysics, Geosystems. 20:5038–5056.
Ingham MR, Bibby HM, Heise W, Jones KA, Cairns P, Dravitzki S, Bennie SL, Caldwell TG, Ogawa Y. 2009. A magnetotelluric study of Mount Ruapehu volcano, New Zealand. Geophysical Journal International. 179:887–904.
Ingham E, Turner GM, Conway CE, Heslop D, Roberts AP, Leonard G, Townsend D, Calvert A. 2017. Volcanic records of the Laschamp geomagnetic excursion from Mt Ruapehu, New Zealand. Earth and Planetary Science Letters. 472:131–141.
Johnson JH, Savage MK. 2012. Tracking volcanic and geothermal activity in the Tongariro Volcanic Centre, New Zealand, with shear wave splitting tomography. Journal of Volcanology and Geothermal Research. 223:1–10.
Johnson JH, Savage MK, Townend J. 2011. Distinguishing between stress-induced and structural anisotropy at Mount Ruapehu volcano, New Zealand. Journal of Geophysical Research. 116:B12303.
Johnston DM, Houghton BF, Neall VE, Ronan KR, Paton D. 2000. Impacts of the 1945 and 1995–1996 Ruapehu eruptions, New Zealand: an example of increasing societal vulnerability. Geological Society of America Bulletin. 112:720–726.
Jolly AD, Cronin SJ. 2014. From eruption to end-user; bridging the science-management interface during the 2012 Te Maari eruption, Tongariro Volcano, New Zealand. Journal of Volcanology and Geothermal Research. 286:183.
Jolly AD, Jousset P, Lyons JJ, Carniel R, Fournier N, Fry B, Miller C. 2014. Seismo-acoustic evidence for an avalanche driven phreatic eruption through a beheaded hydrothermal system: an example from the 2012 Tongariro eruption. Journal of Volcanology and Geothermal Research. 286:331–347.
Jolly AD, Neuberg J, Jousset P, Sherburn S. 2012. A new source process for evolving repetitious earthquakes at Ngauruhoe volcano, New Zealand. Journal of Volcanology and Geothermal Research. 215:26–39.

Jolly AD, Sherburn S, Jousset P, Kilgour G. 2010. Eruption source processes derived from seismic and acoustic observations of the 25 September 2007 Ruapehu eruption—North Island, New Zealand. Journal of Volcanology and Geothermal Research. 191:33–45.

Jones KA, Ingham MR, Bibby HM. 2008. The hydrothermal vent system of Mount Ruapehu, New Zealand—a high frequency MT survey of the summit plateau. Journal of Volcanology and Geothermal Research. 176:591–600.

Kereszturi G, Schaefer LN, Miller C, Mead S. 2020. Hydrothermal alteration on composite volcanoes: mineralogy, hyperspectral imaging and aeromagnetic study of Mt Ruapehu, New Zealand. Geochemistry, Geophysics, Geosystems. 21:e2020GC009270.

Keys HJ. 2007. Lahars of Ruapehu volcano, New Zealand: risk mitigation. Annals of Glaciology. 45:155–162.

Keys HJR, Green PM. 2010. Mitigation of volcanic risks at Mt Ruapehu, New Zealand. In Proceedings of the Mountain Risks International Conference, Firenze, Italy. CERG, Strasbourg, France. p. 24–26.

Kilgour G, Blundy J, Cashman K, Mader HM. 2013. Small volume andesite magmas and melt–mush interactions at Ruapehu, New Zealand: evidence from melt inclusions. Contributions to Mineralogy and Petrology. 166:371–392.

Kilgour G, Manville V, Della Pasqua F, Graettinger A, Hodgson KA, Jolly GE. 2010. The 25 September 2007 eruption of Mount Ruapehu, New Zealand: directed ballistics, surtseyan jets, and ice-slurry lahars. Journal of Volcanology and Geothermal Research. 191:1–14.

Kilgour GN, Saunders KE, Blundy JD, Cashman KV, Scott BJ, Miller CA. 2014. Timescales of magmatic processes at Ruapehu volcano from diffusion chronometry and their comparison to monitoring data. Journal of Volcanology and Geothermal Research. 288:62–75.

Kósik S, Németh K, Kereszturi G, Procter JN, Zellmer GF, Geshi N. 2016. Phreatomagmatic and water-influenced Strombolian eruptions of a small-volume parasitic cone complex on the southern ringplain of Mt. Ruapehu, New Zealand: facies architecture and eruption mechanisms of the Ohakune Volcanic Complex controlled by an unstable fissure eruption. Journal of Volcanology and Geothermal Research. 327:99–115.

Latter JH. 1981. Volcanic earthquakes, and their relationship to eruptions at Ruapehu and Ngauruhoe volcanoes. Journal of Volcanology and Geothermal Research. 9:293–309.

Le Bas MJ, Le Maitre RW, Streckeisen A, Zanettin B. 1986. A chemical classification of volcanic rocks based on the total alkali–silica diagram. Journal of Petrology. 27:745–750.

Lecointre J, Hodgson K, Neall V, Cronin S. 2004. Lahar-triggering mechanisms and hazard at Ruapehu volcano, New Zealand. Natural Hazards. 31:85–109.

Lecointre JA, Neall VE, Palmer AS. 1998. Quaternary lahar stratigraphy of the western Ruapehu ring plain, New Zealand. New Zealand Journal of Geology and Geophysics. 41:225–245.

Lecointre JA, Neall VE, Wallace CR, Prebble WM. 2002. The 55-to 60-ka Te Whaiau Formation: a catastrophic, avalanche-induced, cohesive debris-flow deposit from proto-Tongariro volcano, New Zealand. Bulletin of Volcanology. 63:509–525.

Leonard GS, Johnston DM, Paton D, Christianson A, Becker J, Keys H. 2008. Developing effective warning systems: ongoing research at Ruapehu volcano, New Zealand. Journal of Volcanology and Geothermal Research. 172:199–215.

Leonard GS, Stewart C, Wilson TM, Procter JN, Scott BJ, Keys HJ, Jolly GE, Wardman JB, Cronin SJ, McBride SK. 2014. Integrating multidisciplinary science, modelling and impact data into evolving, syn-event volcanic hazard mapping and communication: a case study from the 2012 Tongariro eruption crisis, New Zealand. Journal of Volcanology and Geothermal Research. 286:208–232.

Lisiecki LE, Raymo ME. 2005. A Pliocene-Pleistocene stack of 57 globally distributed benthic $\delta^{18}O$ records. Paleoceanography. 20:PA1003.

Liu J, Salmond JA, Dirks KN, Lindsay JM. 2015. Validation of ash cloud modelling with satellite retrievals: a case study of the 16–17 June 1996 Mount Ruapehu eruption. Natural Hazards. 78:973–993.

Lube G, Breard EC, Cronin SJ, Procter JN, Brenna M, Moebis A, Pardo N, Stewart RB, Jolly A, Fournier N. 2014. Dynamics of surges generated by hydrothermal blasts during the 6 August 2012 Te Maari eruption, Mt. Tongariro, New Zealand. Journal of Volcanology and Geothermal Research. 286:348–366.

Lube G, Cronin SJ, Procter JN. 2009. Explaining the extreme mobility of volcanic ice-slurry flows, Ruapehu volcano, New Zealand. Geology. 37:15–18.

Manville V. 2004. Palaeohydraulic analysis of the 1953 Tangiwai lahar: New Zealand's worst volcanic disaster. Acta Vulcanologica. 16:137–152.

Manville V, Cronin SJ. 2007. Breakout lahar from New Zealand's crater lake. Eos. Transactions of the American Geophysical Union. 88:441–442.

McClelland E, Erwin PS. 2003. Was a dacite dome implicated in the 9,500 BP collapse of Mt Ruapehu? A palaeomagnetic investigation. Bulletin of Volcanology. 65:294–305.

Milicich SD, Chambefort I, Wilson CJN, Alcaraz S, Ireland TR, Bardsley C, Simpson MP. 2020. A zircon U-Pb geochronology for the Rotokawa geothermal system, New Zealand, with implications for Taupō Volcanic Zone evolution. Journal of Volcanology and Geothermal Research. 389:106729.

Miller CA, Currenti G, Hamling I, Williams-Jones G. 2018b. Mass transfer processes in a post eruption hydrothermal system: parameterisation of microgravity changes at Te Maari craters, New Zealand. Journal of Volcanology and Geothermal Research. 357:39–55.

Miller CA, Kang SG, Fournier D, Hill G. 2018a. Distribution of vapor and condensate in a hydrothermal system: insights from self-potential inversion at Mount Tongariro, New Zealand. Geophysical Research Letters. 45:8190–8198.

Miller CA, Schaefer LN, Kereszturi G, Fournier D. 2020. Three dimensional mapping of Mt Ruapehu volcano, New Zealand, from aeromagnetic data inversion and hyperspectral imaging. Journal of Geophysical Research: Solid Earth. 125:e2019JB018247.

Miller CA, Williams-Jones G. 2016. Internal structure and volcanic hazard potential of Mt Tongariro, New Zealand, from 3D gravity and magnetic models. Journal of Volcanology and Geothermal Research. 319:12–28.

Moebis A, Cronin SJ, Neall VE, Smith IE. 2011. Unravelling a complex volcanic history from fine-grained, intricate Holocene ash sequences at the Tongariro Volcanic Centre, New Zealand. Quaternary International. 246:352–363.

Mortimer N. 2004. New Zealand's geological foundations. Gondwana Research. 7:261–272.

Mortimer N, Tulloch AJ, Ireland TR. 1997. Basement geology of Taranaki and Wanganui Basins, New Zealand. New Zealand Journal of Geology and Geophysics. 40:223–236.

Nairn IA, Kobayashi T, Nakagawa M. 1998. The ~10 ka multiple vent pyroclastic sequence at Tongariro Volcanic Centre, Taupo Volcanic Zone, New Zealand. Part 1. Eruptive process during regional extension. Journal of Volcanology and Geothermal Research. 86:19–44.

Nairn IA, Self S. 1978. Explosive eruptions and pyroclastic avalanches from Ngauruhoe in February 1975. Journal of Volcanology and Geothermal Research. 3:39–60.

Nakagawa M, Nairn IA, Kobayashi T. 1998. The~ 10 ka multiple vent pyroclastic eruption sequence at Tongariro Volcanic Centre, Taupo Volcanic Zone, New Zealand: Part 2. Petrological insights into magma storage and transport during regional extension. Journal of Volcanology and Geothermal Research. 86:45–65.

Nakagawa M, Wada K, Thordarson T, Wood CP, Gamble JA. 1999. Petrologic investigations of the 1995 and 1996 eruptions of Ruapehu volcano, New Zealand: formation of discrete and small magma pockets and their intermittent discharge. Bulletin of Volcanology. 61:15–31.

Nakagawa M, Wada K, Wood CP. 2002. Mixed magmas, mush chambers and eruption triggers: evidence from zoned clinopyroxene phenocrysts in andesitic scoria from the 1995 eruptions of Ruapehu volcano, New Zealand. Journal of Petrology. 43:2279–2303.

Newhall CG, Self S. 1982. The volcanic explosivity index (VEI) an estimate of explosive magnitude for historical volcanism. Journal of Geophysical Research. 87:1231–1238.

Newnham RM, Dirks KN, Samaranayake D. 2010. An investigation into long-distance health impacts of the 1996 eruption of Mt Ruapehu, New Zealand. Atmospheric Environment. 44:1568–1578.

Palmer BA, Neall VE. 1989. The Murimotu formation—9500 year old deposits of a debris avalanche and associated lahars, Mount Ruapehu, North Island, New Zealand. New Zealand Journal of Geology and Geophysics. 32:477–486.

Pardo N, Cronin SJ, Palmer AS, Németh K. 2012a. Reconstructing the largest explosive eruptions of Mt. Ruapehu, New Zealand: lithostratigraphic tools to understand subplinian–plinian eruptions at andesitic volcanoes. Bulletin of Volcanology. 74:617–640.

Pardo N, Cronin S, Palmer A, Procter J, Smith I. 2012b. Andesitic Plinian eruptions at Mt. Ruapehu: quantifying the uppermost limits of eruptive parameters. Bulletin of Volcanology. 74:1161–1185.

Pardo N, Cronin SJ, Wright HM, Schipper CI, Smith I, Stewart B. 2014. Pyroclast textural variation as an indicator of eruption column steadiness in andesitic Plinian eruptions at Mt. Ruapehu. Bulletin of Volcanology. 76:822.

Park I, Jolly A, Kim KY, Kennedy B. 2019. Temporal variations of repeating low frequency volcanic earthquakes at Ngauruhoe Volcano, New Zealand. Journal of Volcanology and Geothermal Research. 373:108–119.

Paton D, Johnston D, Houghton BF. 1998. Organisational response to a volcanic eruption. Disaster Prevention and Management. 7:5–13.

Potter SH, Jolly GE, Neall VE, Johnston DM, Scott BJ. 2014. Communicating the status of volcanic activity: revising New Zealand's volcanic alert level system. Journal of Applied Volcanology. 3:13.

Price RC, Gamble JA, Smith IEM, Maas R, Waight T, Stewart RB, Woodhead J. 2012. The anatomy of an andesite volcano: a time-stratigraphic study of andesite petrogenesis and crustal evolution at Ruapehu Volcano, New Zealand. Journal of Petrology. 53:2139–2189.

Price RC, Gamble JA, Smith IEM, Stewart RB, Eggins SM, Wright IC. 2005. An integrated model for the temporal evolution of andesites and rhyolites and crustal development in New Zealand's North Island. Journal of Volcanology and Geothermal Research. 140:1–24.

Price RC, Turner S, Cook C, Hobden B, Smith IEM, Gamble JA, Handley H, Maas R, Möbis A. 2010. Crustal and mantle influences and U–Th–Ra disequilibrium in andesitic lavas of Ngauruhoe Volcano, New Zealand. Chemical Geology. 277:355–373.

Procter JN, Cronin SJ, Fuller IC, Sheridan M, Neall VE, Keys H. 2010. Lahar hazard assessment using Titan2D for an alluvial fan with rapidly changing geomorphology: Whangaehu River, Mt. Ruapehu. Geomorphology. 116:162–174.

Procter JN, Cronin SJ, Sheridan MF. 2012. Evaluation of Titan2D modelling forecasts for the 2007 Crater Lake break-out lahar, Mt. Ruapehu, New Zealand. Geomorphology. 136:95–105.

Procter JN, Cronin SJ, Zernack AV, Lube G, Stewart RB, Nemeth K, Keys H. 2014. Debris flow evolution and the activation of an explosive hydrothermal system; Te Maari, Tongariro, New Zealand. Journal of Volcanology and Geothermal Research. 286:303–316.

Pruess K. 1991. TOUGH2—A general-purpose numerical simulator for multiphase fluid and heat flow. Report LBL-29400. Lawrence Berkeley National Laboratory.

Pure LR. 2020. The volcanic and magmatic evolution of Tongariro Volcano, New Zealand. [PhD Thesis]. Wellington, New Zealand: Victoria University of Wellington, 416 p.

Pure LR, Leonard GS, Townsend DB, Wilson CJN, Calvert AT, Cole RP, Conway CE, Gamble JA, Smith TB. 2020. A high resolution $^{40}Ar/^{39}Ar$ lava chronology and edifice construction history for Tongariro Volcano, New Zealand. Journal of Volcanology and Geothermal Research. 402:106993.

Reyners M, Eberhart-Phillips D, Stuart G, Nishimura Y. 2006. Imaging subduction from the trench to 300 km depth beneath the central North Island, New Zealand, with V_p and V_p/V_s. Geophysical Journal International. 165:565–583.

Robertson E, Davey F. 2018. The basement morphology under Tongariro National Park, southern Taupo Volcanic Zone. New Zealand Journal of Geology and Geophysics. 61:570–577.

Rowland JV, Sibson RH. 2001. Extensional fault kinematics within the Taupo Volcanic Zone, New Zealand: soft-linked segmentation of a continental rift system. New Zealand Journal of Geology and Geophysics. 44:271–283.

Rowlands DP, White RS, Haines AJ. 2005. Seismic tomography of the Tongariro volcanic centre, New Zealand. Geophysical Journal International. 163:1180–1194.

Schaefer LN, Kennedy BM, Villeneuve MC, Cook SC, Jolly AD, Keys HJ, Leonard GS. 2018. Stability assessment of the Crater lake/Te Wai-ā-moe overflow channel at Mt. Ruapehu (New Zealand), and implications for volcanic lake break-out triggers. Journal of Volcanology and Geothermal Research. 358:31–44.

Scott BJ. 2013. A revised catalogue of Ruapehu volcano eruptive activity: 1830-2012. Lower Hutt, NZ: GNS Science. GNS Science Report 2013/45. 107 p.

Scott BJ, Potter SH. 2014. Aspects of historical eruptive activity and volcanic unrest at Mt. Tongariro, New Zealand: 1846–2013. Journal of Volcanology and Geothermal Research. 286:263–276.

Seebeck H, Nicol A, Giba M, Pettinga J, Walsh J. 2014. Geometry of the subducting Pacific plate since 20 Ma,

Hikurangi margin, New Zealand. Journal of the Geological Society, London. 171:131–143.
Shane P, Doyle LR, Nairn IA. 2008. Heterogeneous andesite–dacite ejecta in 26–16.6 ka pyroclastic deposits of Tongariro volcano, New Zealand: the product of multiple magma-mixing events. Bulletin of Volcanology. 70:517–536.
Shane P, Maas R, Lindsay J. 2017. History of Red Crater volcano, Tongariro Volcanic Centre (New Zealand): abrupt shift in magmatism following recharge and contrasting evolution between neighboring volcanoes. Journal of Volcanology and Geothermal Research. 340:1–15.
Sherburn S, Bryan CJ. 1999. The eruption detection system: Mt. Ruapehu, New Zealand. Seismological Research Letters. 70:505–511.
Sherburn S, Bryan CJ, Hurst AW, Latter JH, Scott BJ. 1999. Seismicity of Ruapehu volcano, New Zealand, 1971-1996: a review. Journal of Volcanology and Geothermal Research. 88:255–278.
Singer BS, Thompson RA, Dungan MA, Feeley TC, Nelson ST, Pickens JC, Brown LL, Wulff AW, Davidson JP, Metzger J. 1997. Volcanism and erosion during the past 930 ky at the Tatara–San Pedro complex, Chilean Andes. Geological Society of America Bulletin. 109:127–142.
Sissons BA, Dibble RR. 1981. A seismic refraction experiment southeast of Ruapehu volcano. New Zealand Journal of Geology and Geophysics. 24:31–38.
Spörli KB, Rowland JV. 2006. 'Column on column' structures as indicators of lava/ice interaction, Ruapehu andesite volcano, New Zealand. Journal of Volcanology and Geothermal Research. 157:294–310.
Stewart C, Johnston DM, Leonard GS, Horwell CJ, Thordarson T, Cronin SJ. 2006. Contamination of water supplies by volcanic ashfall: a literature review and simple impact modelling. Journal of Volcanology and Geothermal Research. 158:296–306.
Strehlow K, Sandri L, Gottsmann JH, Kilgour G, Rust AC, Tonini R. 2017. Phreatic eruptions at crater lakes: occurrence statistics and probabilistic hazard forecast. Journal of Applied Volcanology. 6:4.
Topping WW. 1973. Tephrostratigraphy and chronology of late Quaternary eruptives from the Tongariro Volcanic Centre, New Zealand. New Zealand Journal of Geology and Geophysics. 16:397–423.
Tost M, Cronin SJ. 2015. Linking distal volcaniclastic sedimentation and stratigraphy with the development of Ruapehu volcano, New Zealand. Bulletin of Volcanology. 77:94.
Tost M, Cronin SJ. 2016. Climate influence on volcano edifice stability and fluvial landscape evolution surrounding Mount Ruapehu, New Zealand. Geomorphology. 262:77–90.
Townsend DB, Leonard GS, Conway CE, Eaves SR, Wilson CJN. 2017. Geology of the Tongariro National Park Area. Lower Hutt (NZ): GNS Science. 1 sheet + 109 pp, scale 1:60,000. (GNS Science Geological Map 4).
Turner R, Hurst T. 2001. Factors influencing volcanic ash dispersal from the 1995 and 1996 eruptions of Mount Ruapehu, New Zealand. Journal of Applied Meteorology. 40:56–69.
Turner R, Moore S, Pardo N, Kereszturi G, Uddstrom M, Hurst T, Cronin S. 2014. The use of numerical weather prediction and a Lagrangian transport (NAME-III) and dispersion (ASHFALL) models to explain patterns of observed ash deposition and dispersion following the August 2012 Te Maari, New Zealand eruption. Journal of Volcanology and Geothermal Research. 286:437–451.
Vandergoes, MJ, Hogg, AG, Lowe, DJ, Newnham, RM, Denton, GH, Southon, J, Barrell, DJ, Wilson, CJN, McGlone, MS, Allan, ASR, Almond, PC. 2013. A revised age for the Kawakawa/Oruanui tephra, a key marker for the last glacial maximum in New Zealand. Quaternary Science Reviews. 74:195–201.
Villamor P, Berryman KR. 2006. Evolution of the southern termination of the Taupo Rift, New Zealand. New Zealand Journal of Geology and Geophysics. 49:23–37.
Villamor P, Berryman KR, Ellis SM, Schreurs G, Wallace LM, Leonard GS, Langridge RM, Ries WF. 2017. Rapid evolution of subduction-related continental intraarc rifts: the Taupo Rift, New Zealand. Tectonics. 36:2250–2272.
Voight B, Janda RJ, Glicken H, Douglass PM. 1983. Nature and mechanics of the Mount St Helens rockslide-avalanche of 18 May 1980. Geotechnique. 33:243–273.
Voloschina M, Lube G, Procter J, Moebis A, Timm C. 2020. Lithosedimentological and tephrostratigraphical characterisation of small-volume, low-intensity eruptions: The 1800 years Tufa Trig Formation, Mt. Ruapehu (New Zealand). Journal of Volcanology and Geothermal Research. 401:106987.
Waight TE, Price RC, Stewart RB, Smith IEM, Gamble J. 1999. Stratigraphy and geochemistry of the Turoa area, with implications for andesite petrogenesis at Mt Ruapehu, Taupo Volcanic Zone, New Zealand. Journal of Geology and Geophysics. 42:513–532.
Walsh FD, Hochstein MP, Bromley CJ. 1998. The Tongariro geothermal system (NZ): review of geophysical data. In: Simmons SF, Morgan OE, Dunstall MG (compilers). Proceedings of the 20th New Zealand Geothermal Workshop 1998. Auckland, NZ. University of Auckland. 317–324.
Walsh B, Jolly AD, Procter JN. 2016. Seismic analysis of the 13 October 2012 Te Maari, New Zealand, lake breakout lahar: insights into flow dynamics and the implications on mass flow monitoring. Journal of Volcanology and Geothermal Research. 324:144–155.
Wilson CJN. 1993. Stratigraphy, chronology, styles and dynamics of late Quaternary eruptions from Taupo volcano, New Zealand. Philosophical Transactions of the Royal Society of London. A343:205–306.
Wilson SH. 1960. Appendix 3. Physical and chemical investigation of Ketetahi hot springs. In: Gregg DR, Grange LI, Williamson JH, Hurst JA, Clark RH, Wilson SH. The geology of Tongariro subdivision. Lower Hutt, New Zealand Geological Survey. New Zealand Geological Survey Bulletin 40:124–144.
Wilson TM, Cole JW. 2007. Potential impact of ash eruptions on dairy farms from a study of the effects on a farm in eastern Bay of Plenty, New Zealand: implications for hazard mitigation. Natural Hazards. 43:103–128.
Wilson CJN, Houghton BF, McWilliams MO, Lanphere MA, Weaver SD, Briggs RM. 1995. Volcanic and structural evolution of Taupo Volcanic Zone, New Zealand: a review. Journal of Volcanology and Geothermal Research. 68:1–28.